The drift history of Iran from the Ordovician to the Triassic

Giovanni Muttoni, Massimo Mattei, Marco Balini, Andrea Zanchi, Maurizio Gaetani and Fabrizio Berra

Geological Society, London, Special Publications 2009; v. 312; p. 7-29
doi:10.1144/SP312.2

The drift history of Iran from the Ordovician to the Triassic

GIOVANNI MUTTONI[1]*, MASSIMO MATTEI[2], MARCO BALINI[1], ANDREA ZANCHI[3], MAURIZIO GAETANI[1] & FABRIZIO BERRA[1]

[1]*Dipartimento di Scienze della Terra, Università di Milano, via Mangiagalli 34, I-20133 Milano, Italy, and ALP – Alpine Laboratory of Paleomagnetism, via Madonna dei Boschi 76, I-12016 Peveragno (CN), Italy*

[2]*Dipartimento di Scienze Geologiche, Università di Roma-Tre, Largo San Leonardo Murialdo 1, I-00146 Roma, Italy*

[3]*Dipartimento Scienze Geologiche e Geotecnologie, Università di Milano-Bicocca, Piazza della Scienza 4, I-20126 Milano, Italy*

**Corresponding author (e-mail: giovanni.muttoni1@unimi.it)*

Abstract: New Late Ordovician and Triassic palaeomagnetic data from Iran are presented. These data, in conjunction with data from the literature, provide insights on the drift history of Iran as part of Cimmeria during the Ordovician–Triassic. A robust agreement of palaeomagnetic poles of Iran and West Gondwana is observed for the Late Ordovician–earliest Carboniferous, indicating that Iran was part of Gondwana during that time. Data for the Late Permian–early Early Triassic indicate that Iran resided on subequatorial palaeolatitudes, clearly disengaged from the parental Gondwanan margin in the southern hemisphere. Since the late Early Triassic, Iran has been located in the northern hemisphere close to the Eurasian margin. This northward drift brought Iran to cover much of the Palaeotethys in approximately 35 Ma, at an average plate speed of *c.* 7–8 cm year^{-1}, and was in part coeval to the transformation of Pangaea from an Irvingian B to a Wegenerian A-type configuration.

According to Sengör (1979), a strip of Gondwanan terranes called the Cimmerian Continent, which includes Iran, broke off the eastern Gondwanan margin during the Permian–Triassic, drifted northwards across the Palaeotethys in a windscreen-wiper fashion and eventually collided with the Eurasian margin, giving birth to a conspicuous mountain chain, the Cimmerian orogen. This eminent and imaginative model of plates' motion had a profound impact on Tethyan geology and was particularly appealing to palaeomagnetists insofar as it is testable by using the relationship between inclination of the time-averaged geomagnetic field and latitude. Indeed, quoting Van der Voo (1993), 'the observed palaeolatitudes vindicate, in a very convincing way, the model of the Cimmerian continental motion of Sengör & colleagues, at least insofar as Iran is concerned', and this was due largely to the research efforts of Wensink *et al.* (1978), Wensink (1979, 1982, 1983) and, more recently, Besse *et al.* (1998).

This premise would suggest that the drift model of Iran is grounded on a sound palaeomagnetic basis. However, in some instances, palaeomagnetically determined palaeolatitudes could be ambiguous for the reason that, without independent estimates of polarity, the hemisphere of magnetization acquisition is undetermined. This ambiguity was resolved by Besse *et al.* (1998) in the Late Permian–Early Triassic by means of magnetostratigraphic correlations to sections of known polarity, but this exercise of polarity determination remains an exception in the Iranian database. Polarity (hemispheric) uncertainty can represent a problem when attempting to resolve the motion of Iran or other Cimmerian terranes because the Tethys Gulf was largely symmetric with respect to the palaeoequator. In this paper, new palaeomagnetic data from Iran are presented and a critical revision of palaeomagnetic data from the literature is attempted with the aim to refine the drift history of Iran over the Ordovician–Triassic.

Palaeomagnetic data

Palaeomagnetic analyses were conducted on samples from sediments biostratigraphically constrained to the Late Ordovician, Late Permian, Early Triassic and late Early–late Middle Triassic (Olenekian–late Ladinian). Palaeomagnetic samples were drilled in the field with a water-cooled rock drill and oriented

From: BRUNET, M.-F., WILMSEN, M. & GRANATH, J. W. (eds) *South Caspian to Central Iran Basins*. The Geological Society, London, Special Publications, **312**, 7–29.
DOI: 10.1144/SP312.2 0305-8719/09/$15.00

with a magnetic compass. All samples were thermally demagnetized and measured after each heating step on a 2G Enterprises dc SQUID (superconducting quantum interference device) cryogenic magnetometer located in a shielded room at the Alpine Laboratory of Paleomagnetism of Peveragno, Italy. An average of 50 °C steps from room temperature to a maximum of 680 °C were adopted. The component structure of the natural remanent magnetization (NRM) was monitored after each demagnetization step by means of vector end-point demagnetization diagrams (Zijderveld 1967), and steps of 25–10 °C were adopted close to critical unblocking temperatures. Magnetic components were obtained by standard least-square analysis (Kirschvink 1980) on linear portions of the demagnetization paths and plotted on equal-area projections. Standard Fisher (1953) statistics was applied to calculate site mean directions. Inclination-only statistics (McFadden & Reid 1982) were occasionally applied to sites characterized by declination scattering. The magnetic mineralogy of rocks was studied by means of isothermal remanent magnetization (IRM) acquisition curves, thermal decay of a three-component IRM (Lowrie 1990) acquired in 2.5 T (high), 0.5 T (medium) and 0.15 T (low) fields, or simply by analysis of the maximum unblocking temperatures of the NRM.

Upper Ordovician Shirgesht Formation, Anarak

A well-exposed Ordovician–Permian section crops out to the east of the town of Anarak at the edge of the Kavir loot (Sharkovski *et al.* 1984). The sampled site (Fig. 1, site IR12; 33.18°N, 53.89°E) is located at the base of lithological interval 3 of Sharkovski *et al.* (1984) and consists of strata dipping to the SW by 60–70°. They include red bioclastic sandy–silty limestones, silty marls and red shales pertaining to the first marine intercalation of the Shirgesht Formation. Schallreuter *et al.* (2006) attributed this interval to the Late Ordovician based on ostracoda biostratigraphy. Deformation in this general area took place broadly during the Mesozoic. The Neo-Cimmerian event is clearly recorded by a strong angular unconformity, metamorphism and the emplacement of magmatic bodies occurring between the Middle–Late Jurassic and the beginning of the Cretaceous. The possible occurrence of Late Triassic

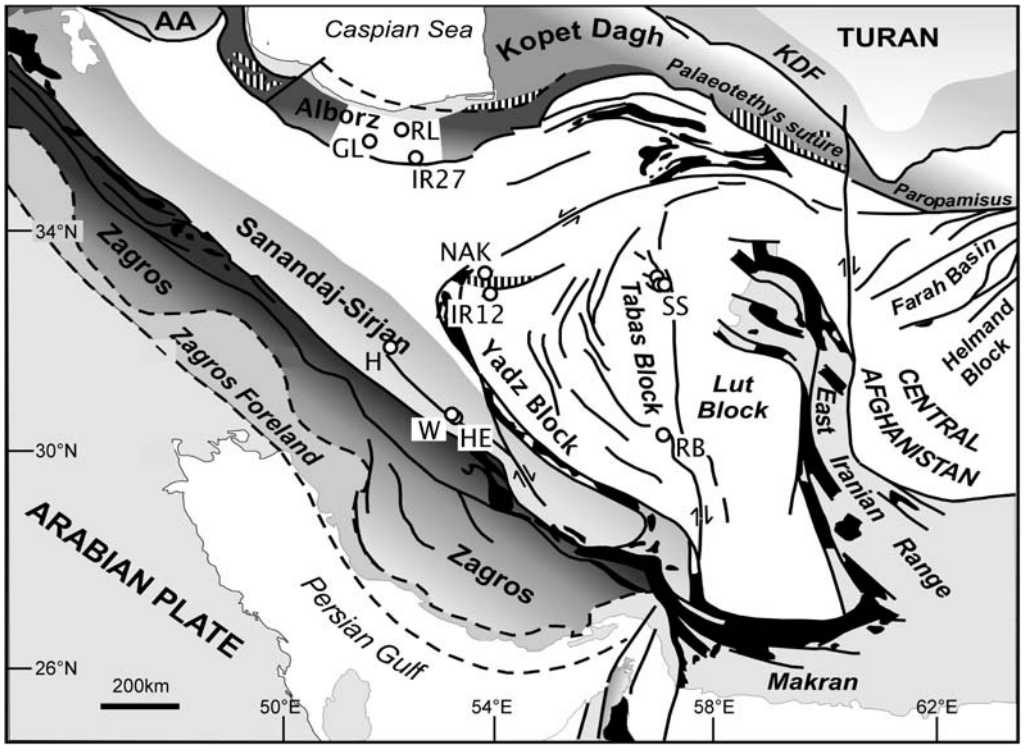

Fig. 1. Structural sketch map of Iran with palaeomagnetic sites discussed in the text indicated. Modified after Angiolini *et al.* (2007).

Eo-Cimmerian compression is discussed by Zanchi *et al.* (2009*b*).

A total of 19 samples have been cored in the field, yielding 28 standard (*c.* 11 cm^3) specimens for palaeomagnetic analyses. Isothermal remanent magnetization acquisition curves show the occurrence of a high coercivity magnetic phase with a tendency to saturate only in fields higher than about 1.5 T (Fig. 2A, left panel). Thermal decay of the NRM shows that this phase consists essentially of hematite characterized by a narrow spectrum of maximum unblocking temperatures around approximately 660–680 °C (Fig. 2A, right panel). Most of the samples show the presence of pervasive A components with northerly and steep down directions in *in situ* co-ordinates (declination (Dec.) = 2.1°E, inclination (Inc.) = 54.3°, Fisher precision parameter (k) = 79.9, Fisher angle of half-cone of 95% confidence about the mean direction (α_{95}) = 3.3°) isolated between room temperature and approximately 175 °C (Fig. 3A, B and Table 1). These components are rather well defined (overall mean angular deviation (MAD) = 2.2°, standard deviation (St) = 2.1°) and are broadly aligned along a recent geocentric axial dipole (GAD) field direction (GAD inclination = 52°). In the temperature range between about 200 and *c.* 675 °C, characteristic C components are observed trending to the origin of the demagnetization axes with well-defined directions (overall MAD = 4.7°, St = 2.1°) oriented northeasterly and steeply down, which, upon correction for bedding tilt, become westerly and steeply down (Dec. = 263.0°E, Inc. = 51.8°, k = 47.2, α_{95} = 4.2°; Fig. 3A, B and Table 1). No field test is available to constrain the age of these C components, which are nonetheless regarded as primary (Late Ordovician) based on palaeomagnetic poles analysis, as discussed in the next section.

Upper Permian Aruh laterite

A lateritic residual profile crops out near the Aruh village in the Alborz Mountains of north Iran (Fig. 1, site IR27; 35.66°N, 52.40°E). Age, chemical composition, palaeomagnetic properties and palaeogeographic implications of this residual profile and similar deposits from other Cimmerian units are discussed in Muttoni *et al.* (submitted). In brief, this profile is Late Permian in age, and is comprised between the carbonate platform limestones of the Ruteh Formation of Middle Permian (Capitanian) age and the carbonate platform limestones of the Elikah Formation of early Early Triassic (Induan) age (Gaetani *et al.* 2009 and references therein). The lowermost part of the profile consists of approximately 1 m of quartz-rich conglomerates and quartz arenites in a red shaly matrix, overlain by *c.* 16 m of yellowish–brown laminated marls and fine-grained oolitic limestones. A laterally discontinuous 3–5 m-thick red–brown, fine-grained and massive bed overturned and dipping to the north by approximately 77° is present in this interval, and will hereafter be referred to as Aruh laterite. At the top, the residual profile grades into the marls and limestones of the basal Elikah Formation. Deformation in this general area took place essentially during the Cenozoic (e.g. Allen *et al.* 2003), although the effects of older deformational phases since the Late Triassic–Early Jurassic Eo-Cimmerian orogeny cannot be excluded. The studied site is located along the southern flank of a late Cenozoic anticline, which is crossed by the Mosha Fault, an active left-lateral strike-slip fault with large displacement (Allen *et al.* 2003).

A total of 18 samples have been cored in the field in the Aruh laterite, yielding an equivalent amount of approximately 11 cm^3 specimens for palaeomagnetic analyses. The Aruh laterite contains hematite of chemical origin that carries essentially two (and rarely three) magnetic components. Components oriented broadly along a recent GAD field direction in *in situ* co-ordinates dominate from room temperature up to about 250 °C. Characteristic C components (MAD = 4.7°, St = 3.5°) are isolated in the *c.* 350–620 °C temperature range. These are orientated essentially west and up in *in situ* co-ordinates, or NW and very shallow upon correction for bedding tilt (Dec. = 331.8°E, Inc. = −1.3°, k = 18.5, α_{95} = 10.4°; Table 1) (see in Muttoni *et al.*, submitted, for additional information). No field test is available to constrain the age of these C components, but, as for data from the Shirgesht Formation, we propose a primary (Late Permian) age of magnetization based on palaeogeographic considerations as discussed in the following section and in Muttoni *et al.* (submitted).

Lower Triassic Sorkh Shale, Tabas

Thin-bedded reddish oolitic–bioclastic limestones and marly limestones pertaining to the Sorkh Shale are exposed in the Shotori Range near the town of Tabas (Fig. 1, site SS). These sediments are Early Triassic in age (Brönnimann *et al.* 1973) and have previously been studied for palaeomagnetism by Wensink (1982). In this same area we sampled two sites, namely IR34 (33.29°N, 57.37°E) and IR35 (33.37°N, 57.25°E), which yielded 19 and 21 standard *c.* 11 cm^3 specimens for palaeomagnetic analyses, respectively. At both sites bedding attitude is highly variable, with strata dipping to the SE by approximately 60–85° at site IR34, and to the SSW by approximately 55–75° at site IR35. Both sites are located along the northern branch of the North–South Nayband

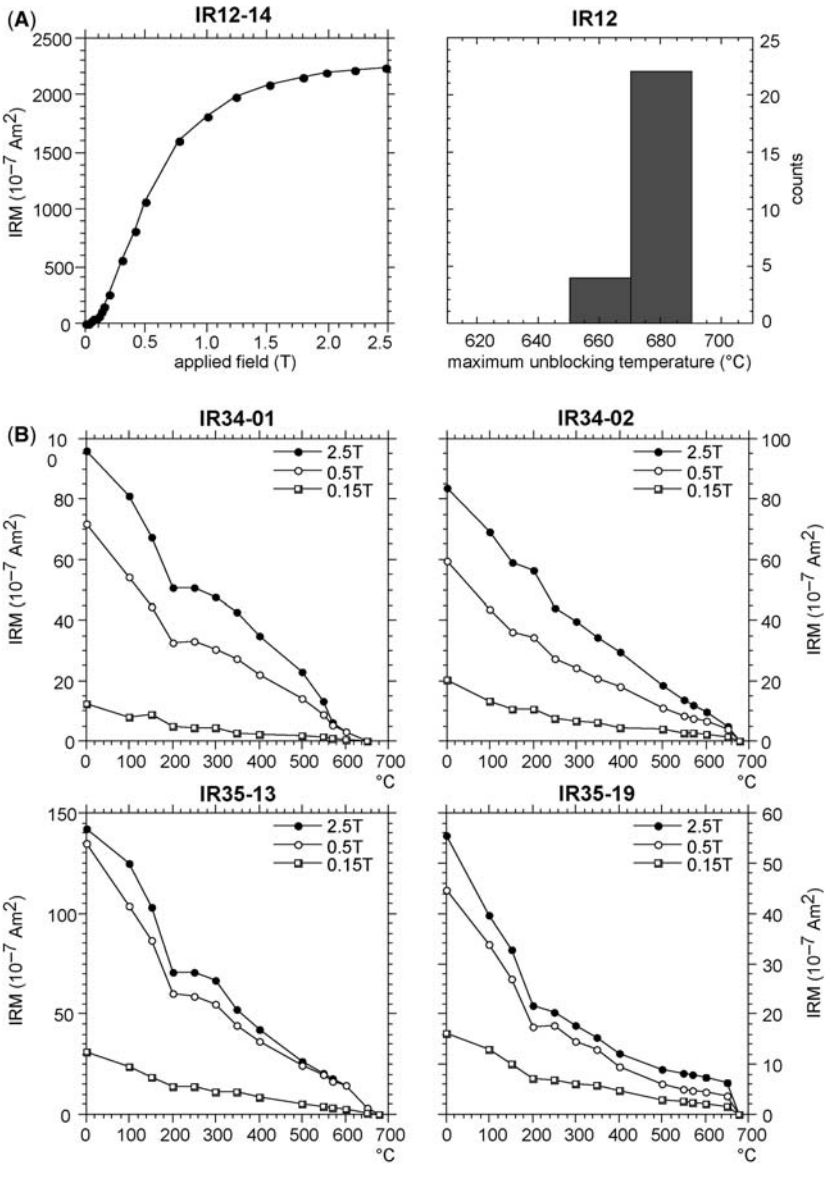

Fig. 2. Rock magnetic experiments on representative samples from this study. (**A**) Isothermal remanent magnetization (IRM) acquisition curve of sample IR12-14 from Upper Ordovician site IR12 (left panel) and histogram of maximum unblocking temperatures of the natural remanent magnetization (NRM) of samples from site IR12 (right panel). (**B**) Thermal decay of a three-component IRM (Lowrie 1990) acquired in 2.5 T (high), 0.5 T (medium) and 0.15 T (low) fields in samples from sites IR34 and IR35 from the Lower Triassic Sorkh Shale. (**C**) Thermal decay of a three-component IRM (same as in (C)) of samples from sites IR02 and IR04 from late Early Triassic (Olenekian) nodular limestones from Nakhlak; histograms of maximum unblocking temperatures of the NRM of samples from sites IR03 and IR17 (left panel), and IR01 and IR05 (right panel), from volcanoclastic sandstones from Nakhlak.

Fault, an active dextral strike-slip structure associated with complex folding.

Thermal decay of the three-component IRM show that samples from both sites contain essentially hematite with maximum unblocking temperatures approaching *c.* 680 °C; medium–high coercivity minerals with unblocking temperatures around 150–200 °C are also present and interpreted as iron hydroxide phases (Fig. 2B). Thermal decay of the NRM reveals the presence in most of the

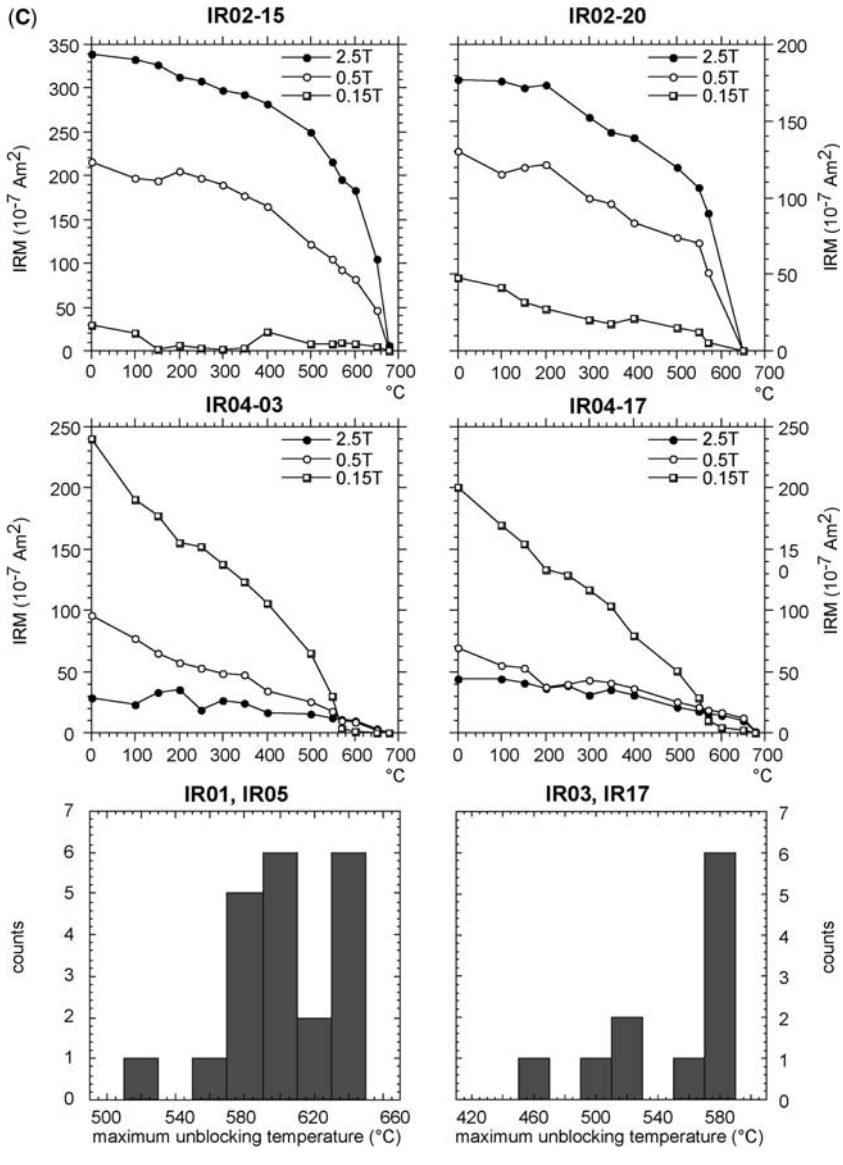

Fig. 2. *Continued.*

samples from site IR34 of A component directions (MAD = 5.6°, St = 2.1°) isolated between approximately 100 and 320 °C. These are oriented northerly and steep down in *in situ* co-ordinates (Dec. = 351.3°E, Inc. = 55.9°, $k = 46.7$, $\alpha_{95} = 5.7°$), and are distributed broadly around a recent GAD field direction (GAD inclination = 53°). In samples from site IR35, similar components (MAD = 5.4°, St = 2.1°) with *in situ* GAD-aligned directions (Dec. = 4.6°E, Inc. = 48.3°, $k = 99.3$, $\alpha_{95} = 3.6°$) are present between room temperature and approximately 250 °C (Fig. 4A, B and Table 1). Removal of these A components reveals the presence of characteristic C components isolated between approximately 450 and 650 °C at site IR34 (MAD = 2.5°, St = 1.1°), and approximately 525–660 °C at site IR35 (MAD = 2.6°, St = 1.3°). The boundary between low-temperature A and high-temperature C components at both sites is frequently transitional, with directions moving along small-circle paths. The C components at both sites show high degrees of dispersion, but, after correction for

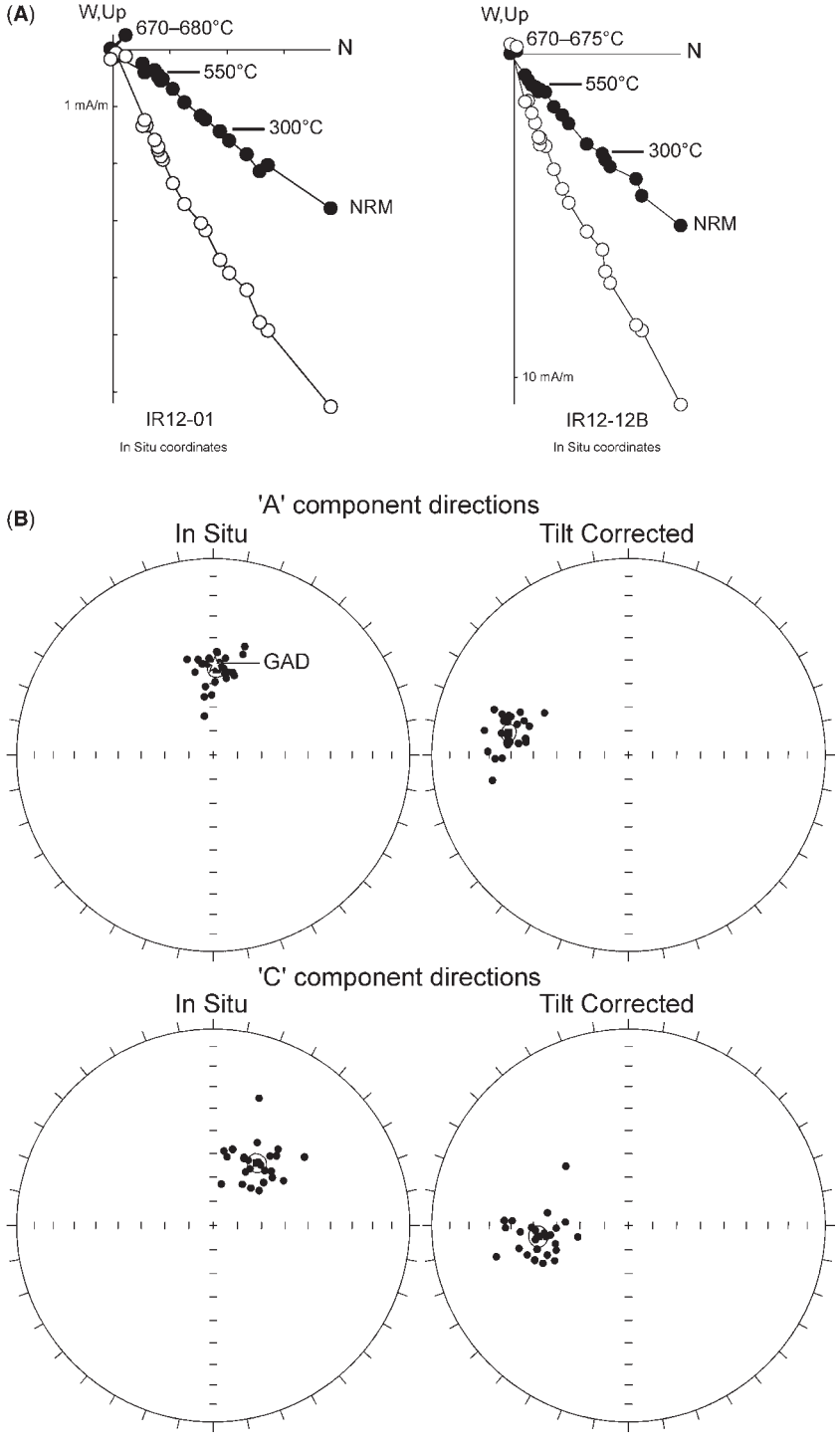

Fig. 3. Palaeomagnetic data from the Upper Ordovician Shirgesht Formation of site IR12. (**A**) Vector end-point demagnetization diagrams of samples IR12-01 and IR12-12B. Closed symbols are projections onto the horizontal plane and open symbols onto the vertical plane in *in situ* (geographical) co-ordinates. Demagnetization temperatures are expressed in °C. (**B**) Equal-area projections before (*in situ*) and after bedding tilt correction of the A and C component directions. Closed symbols are projections onto the lower hemisphere and open symbols onto the upper hemisphere.

Table 1. *Palaeomagnetic mean directions from this study*

Comp.	T.unblock	*N*	*In situ*				Tilt corrected			
			k	α_{95}	MGDEC	MGINC	*k*	α_{95}	MBDEC	MBINC
IR12 – Anarak (33.18°N, 53.89°E), Shirgesht Formation, Upper Ordovician										
A	*c.* 030–175	24	79.9	3.3	2.1	54.3	78.1	3.4	280.5	38.0
C	*c.* 200–675	26	52.6	3.9	35.0	58.2	47.2	4.2	263.0	51.8
IR27 – Aruh Laterite (35.66°N, 52.40°E), Upper Permian (Muttoni *et al.* submitted)										
A	*c.* 100–250	8	134.2	4.8	2.7	52.9	134.7	4.8	198.0	23.7
B1	*c.* 100–325	4	70.3	11.0	299.9	81.9	70.3	11.0	199.7	−10.4
C	*c.* 350–620	12	18.5	10.4	265.1	−47.8	18.5	10.4	331.8	−1.3
IR34 – Tabas (33.29°N, 57.37°E), Sorkh Shale, Lower Triassic										
A	*c.* 100–320	15	46.7	5.7	351.3	55.9	41.1	6.0	105.5	53.1
C	*c.* 450–650	12	9.4			21.0 ± 15.6	25.3			20.3 ± 9.2
IR35 – Tabas (33.37°N, 57.25°E), Sorkh Shale, Lower Triassic										
A	*c.* 030–250	17	99.3	3.6	4.6	48.3	58.7	4.7	211.1	60.3
C	*c.* 525–660	15	16.1			61.9 ± 9.8	52.2			15.4 ± 5.3
IR34 and IR35 combined (inclination only statistics)										
C	*c.* 450–660	27	4.3			43.4 ± 15.2	36.5			17.6 ± 4.6
IR01 – Nakhlak (33.53°N, 53.84°E), Alam Formation, Olenekian										
A	*c.* 100–450	17	30.6	6.6	10.8	45.6	30.5	6.6	9.9	−11.1
B1	*c.* 450–600	6	8.1	25.1	182.3	−27.1	8.1	25.1	182.1	29.5
IR02 – Nakhlak (33.53°N, 53.84°E), Alam Formation, Olenekian										
A	*c.* 030–350	19	257.0	2.1	0.0	50.6	262.9	2.1	9.5	−13.9
C	*c.* 450–675	11	35.8	7.7	167.2	74.9	33.0	8.1	37.7	33.7
IR04 – Nakhlak (33.58°N, 53.83°E), Alam Formation, Olenekian										
A	*c.* 030–300	11	12.0	13.7	358.4	49.4	12.0	13.7	280.8	59.5
C	*c.* 450–665	14	38.2	6.5	184.5	−4.7	33.9	6.9	169.5	−41.3
IR02 and IR04 combined (inclination only statistics)										
C	*c.* 450–675	25					29.0			37.4 ± 5.4
IR03 – Nakhlak (33.54°N, 53.84°E), Alam Formation, lower–middle Anisian										
A	*c.* 100–300	12	137.0	3.7	355.1	51.2	136.6	3.7	0.4	−11.1
B1	*c.* 325–510	4	84.3	10.1	17.2	−20.5	84.2	10.1	61.2	−79.3
IR17 – Nakhlak (33.54°N, 53.84°E), Alam Formation, lower–middle Anisian										
A	*c.* 100–300	18	54.2	4.7	6.4	47.5	45.0	5.2	18.3	−6.5
B1	*c.* 250–450	10	scattered							
B2	*c.* 450–570	7	41.8	9.4	187.7	37.7	43.6	9.2	110.5	60.2
IR05 – Nakhlak (33.56°N, 53.83°E), Ashin Formation, upper Ladinian										
A	*c.* 100–600	19	117.4	3.1	2.2	55.3	56.8	4.5	18.7	−4.0

Comp., palaeomagnetic component; T.unblock, median values of component unblocking temperature (in °C); *N*, number of standard 11 cm^3 specimens; *k*, α_{95}, Fisher (1953) precision parameter and angle of half-cone of 95% confidence about the mean direction, respectively; MGDEC, MGINC, mean geographical (*in situ*) declination and inclination, respectively; MBDEC, MBINC, mean bedding (tilt corrected) declination and inclination, respectively.

bedding tilt, their inclination values tend to cluster around a mean of 20.3° ± 9.2° at site IR34 and 15.4° ± 5.3° at site IR35, with the precision parameter *k* increasing by a factor of 2.7 and 3.2, respectively (Fig. 4B and Table 1). Combining C components from both sites results in a clustering of their inclination values around an overall mean of 17.6° ± 4.6° after correction for bedding tilt, with the precision parameter increasing by a factor of 8.5 (Fig. 4C and Table 1). C components are therefore regarded as pre-folding in age. The dispersion in declination values that persists in bedding co-ordinates is probably owing to uncertainties in the (simple) tilting correction applied and hence in the assumed deformation history of these highly deformed and fault-bounded outcrops.

Lower–Middle Triassic Alam and Ashin formations, Nakhlak

A sedimentary sequence, late Early–late Middle Triassic (Olenekian–late Ladinian) in age, is exposed in the Nakhlak area of Central Iran (Fig. 1, site NAK; *c.* 33.55°N, *c.* 53.84°E). Six

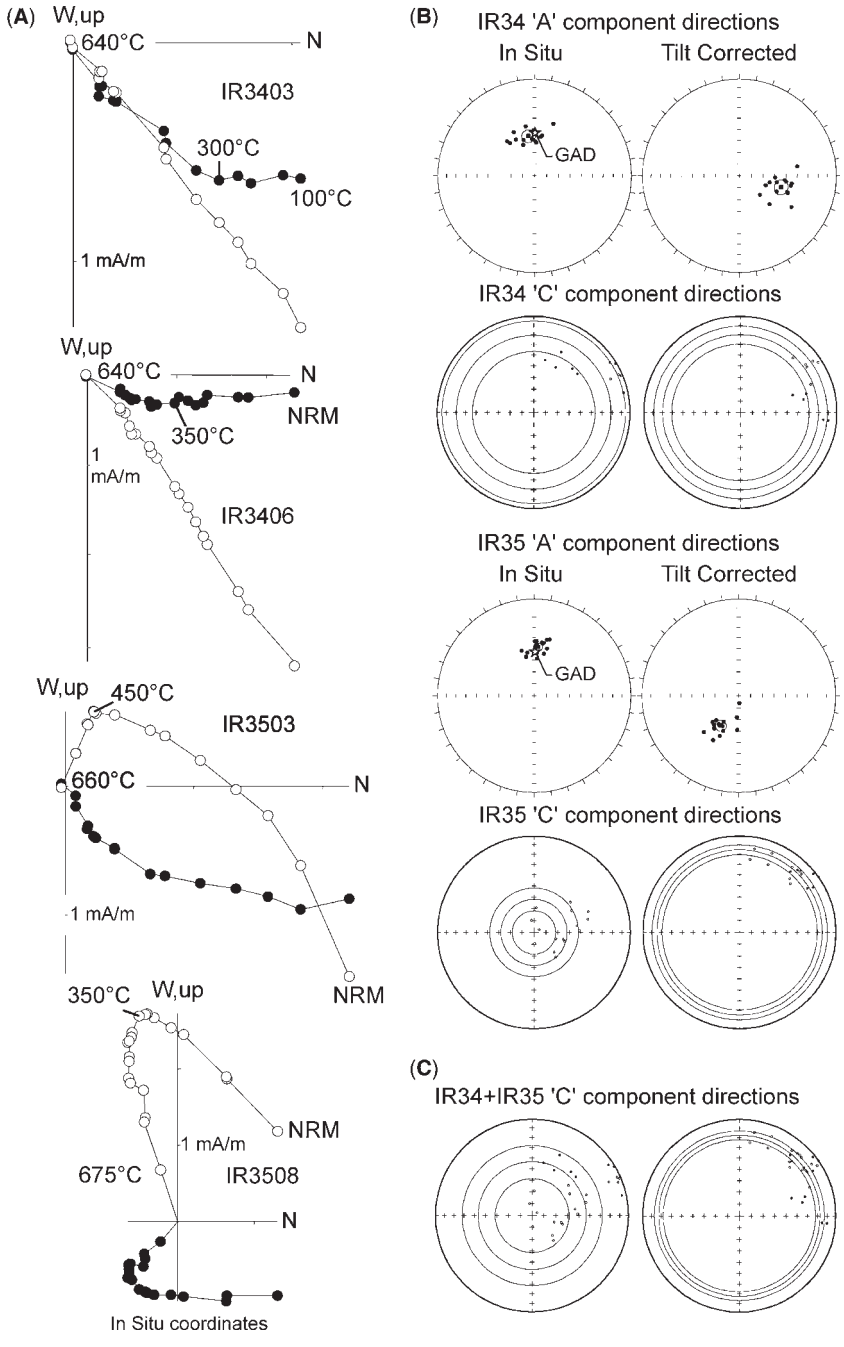

Fig. 4. Palaeomagnetic data from the Lower Triassic Sorkh Shale of sites IR34 and IR35. (**A**) Vector end-point demagnetization diagrams of representative samples from both sites. Closed symbols are projections onto the horizontal plane and open symbols onto the vertical plane in *in situ* (geographical) co-ordinates. Demagnetization temperatures are expressed in °C. (**B**) Equal-area projections before (*in situ*) and after bedding tilt correction of the A and C component directions at both sites; the C components are scattered in declination but show sign of clustering in inclination after correction for bedding tilt. Closed symbols are projections onto the lower hemisphere and open symbols onto the upper hemisphere. (**C**) Equal-area projections before (*in situ*) and after bedding tilt correction of the C component directions of both sites; an improvement in inclination clustering after correction for bedding tilt is evident. Symbols as in (B).

sites (IR01, IR02, IR04, IR03, IR17 and IR05) have been sampled in stratigraphic order from the sequence base to top (Fig. 5A), yielding a total of 109 samples (115 standard, *c.* 11 cm^3, specimens) for palaeomagnetic analyses. The sampled units belong to a geologically complex structure consisting of a WNW–ESE-trending fold-and-thrust belt. Strata at sampling sites generally dip to the NNE by approximately 50°–70°, except for site IR04 where strata dip to the SW by approximately 50°. Gently dipping strata of Upper Cretaceous–Palaeogene limestones and red sandstones unconformably cover the deformed Triassic succession (Zanchi *et al.* 2009*a*). Palaeomagnetic sites consist of volcanoclastic fine-grained sandstones and siltstones, except for sites IR02 and IR04 which consist of reddish nodular limestones. Sites IR01, IR02, IR04, IR03 and IR17 are located in the upper Lower–lower Middle Triassic (Olenekian–middle Anisian) Alam Formation. In particular, sites IR02 and IR04 are located in the Red Nodular Limestone of the Alam Formation, dated to the Olenekian using ammonoid biostratigraphy (Balini *et al.* 2009). Site IR05 is located in the lower part of the Ashin Formation of late Middle Triassic (late Ladinian) age (Balini *et al.* 2009).

These samples contain magnetite and/or hematite in variable proportions. In samples from site IR02, hematite dominates with a narrow spectrum of maximum unblocking temperatures approaching approximately 680 °C, as visible in the thermal decay of the medium–high coercivity components of the IRM (Fig. 2C, samples IR02-15 and IR02-20). In samples from sites IR04, maximum unblocking temperatures consistent with both magnetite (*c.* 570 °C) and hematite coexist, as visible in the thermal decay of the low and medium–high coercivity components of the IRM, respectively (Fig. 2C, samples IR04-03 and IR04-17). Analysis of the maximum unlocking temperatures of the NRM seems also to suggest the coexistence of magnetite and hematite in samples from sites IR01 and IR05, whereas samples from sites IR03 and IR17 appear dominated by magnetite (Fig. 2C, lower panels).

Palaeomagnetic components have been grouped into four categories labelled A, B1, B2 and C. Components A, B1 and B2 are regarded as post-depositional overprints of different origin and age, whereas the characteristic C components are tentatively regarded as primary (syn-depositional) in age, as discussed later. Most of the samples from all sites show the presence of pervasive A components (MAD = 3.5°, St = 2.6°) with northerly and steeply down directions in *in situ* co-ordinates, isolated from room temperature–100 °C to approximately 300–450 °C, occasionally up to about 600 °C (Figs 5B & 6 and Table 1). The A component directions are clearly grouped around a recent GAD field direction in *in situ* co-ordinates (Fig. 5C). The overall mean of $N = 6$ sites (Dec. = 2.3°E, Inc. = 50.1°, $k = 263$, $\alpha_{95} = 4.1°$) is statistically undistinguishable from the local GAD inclination of 53°. Upon correction for bedding tilt, the sites' mean directions become scattered, the overall precision parameter k reducing by a factor of 42 (Fig. 5C).

Removal of these A components reveals the presence in samples from sites IR02 and IR04 of characteristic C component directions (MAD = 7.0°, St = 3.9°) isolated between approximately 400 and 675 °C, and trending to the origin of the demagnetization axes (Figs 5B & 6 and Table 1). At site IR04 these C components show dual polarity. The C component site mean directions are 99.7° apart along a great circle in *in situ* co-ordinates, and after correction for bedding tilt they tend to cluster, reducing their great-circle separation to 38.5° (Fig. 5D). Inclination-only statistics applied to C components from both sites resulted in a clustering of their inclination values around an overall mean of $37.4° \pm 5.4°$ after correction for bedding tilt (Fig. 5D and Table 1).

Finally, B1 and B2 component directions were also observed in samples from sites IR01, IR03 and IR17 in the *c.* 250–600 °C temperature range after removal of the A components (Figs 5B & 6 and Table 1). At site IR01, the B1 components in *in situ* co-ordinates are quasi-antipodal to the *in situ* A components found in the same site at lower temperatures (Fig. 5B). These B1 components may thus represent recent overprints of reverse polarity. For samples from sites IR03 and IR17, the B1 components are more obscure and difficult to interpret. They are not compatible with recent field directions in *in situ* co-ordinates, and their site mean directions show no sign of clustering upon correction for bedding tilt. At site IR17, removal of these B1 components reveals the presence of B2 components with a tilt-corrected mean inclination value of 60.2° ($\alpha_{95} = 9.2°$; Table 1) that is significantly different from, and hence apparently inconsistent with, the inclination values of the characteristic C components isolated at sites IR02 and IR04 (average inclination of 37.4°).

In conclusion, post-depositional remagnetization events of thermochemical origin pervasively overprinted all volcaniclastic sandstone and siltstone samples, generating recent GAD-aligned A components and possibly also scattered B1 and B2 components. Nodular limestones at sites IR02 and IR04 survived overprinting, showing apparently pre-folding C components that are possibly primary (syn-depositional) in age. The dispersion in their site mean declination values that persists after correction for bedding tilt is probably due to

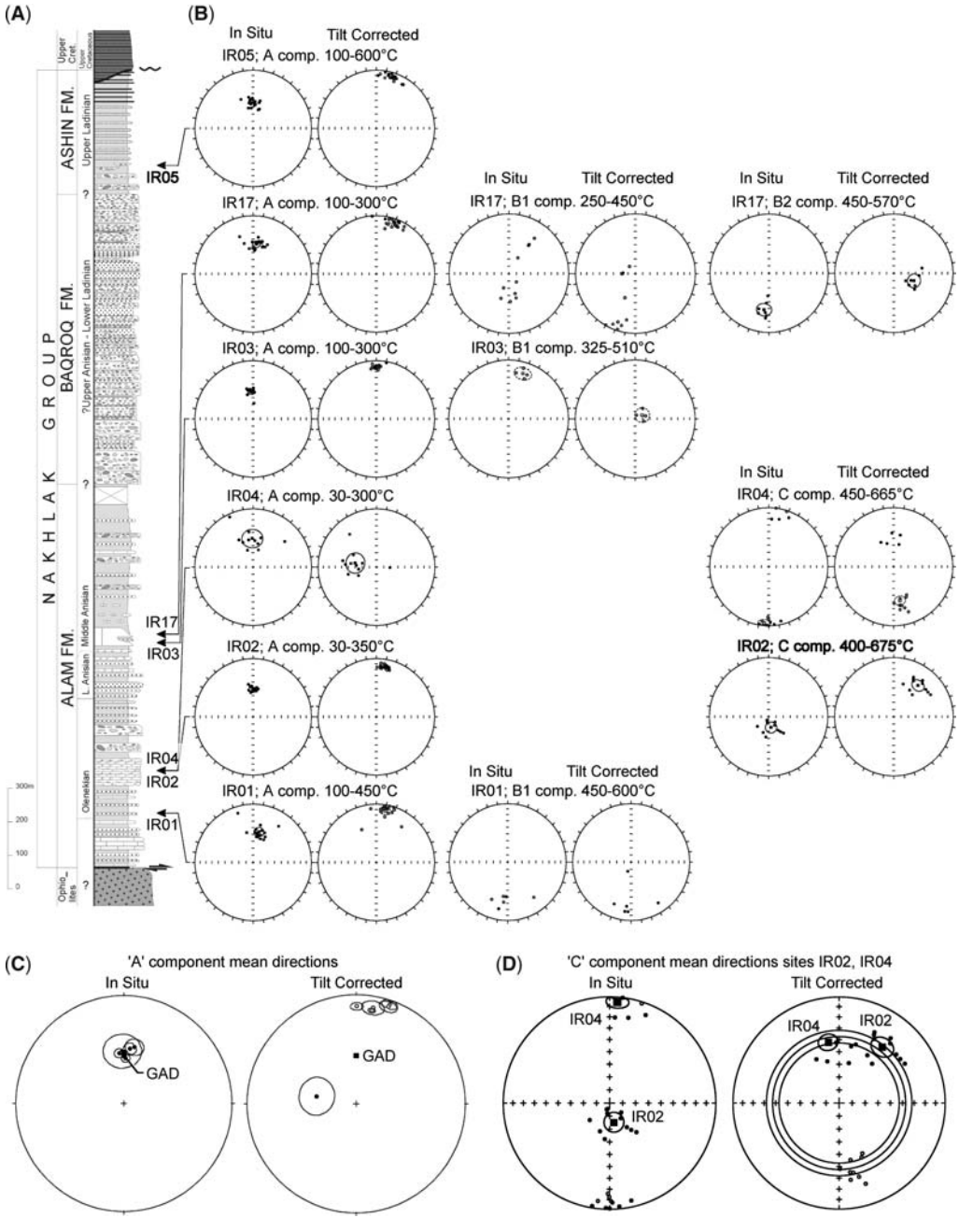

Fig. 5. Stratigraphic and palaeomagnetic data of Triassic sediments from Nakhlak. (**A**) Stratigraphic log with location of palaeomagnetic sampling sites. (**B**) Equal-area projections before (*in situ*) and after bedding tilt correction of the A, B1, B2 and C component directions isolated in each site. (**C**) Equal-area projections before (*in situ*) and after bedding tilt correction of the A component site mean directions, showing an evident grouping along a recent geocentric axial dipole (GAD) field direction in *in situ* co-ordinates. (**D**) Equal-area projections before (*in situ*) and after bedding tilt correction of the C component site mean directions from sites IR02 and IR04, showing a relative improvement in inclination grouping after correction for bedding tilt. Closed symbols are projections onto the lower hemisphere and open symbols onto the upper hemisphere.

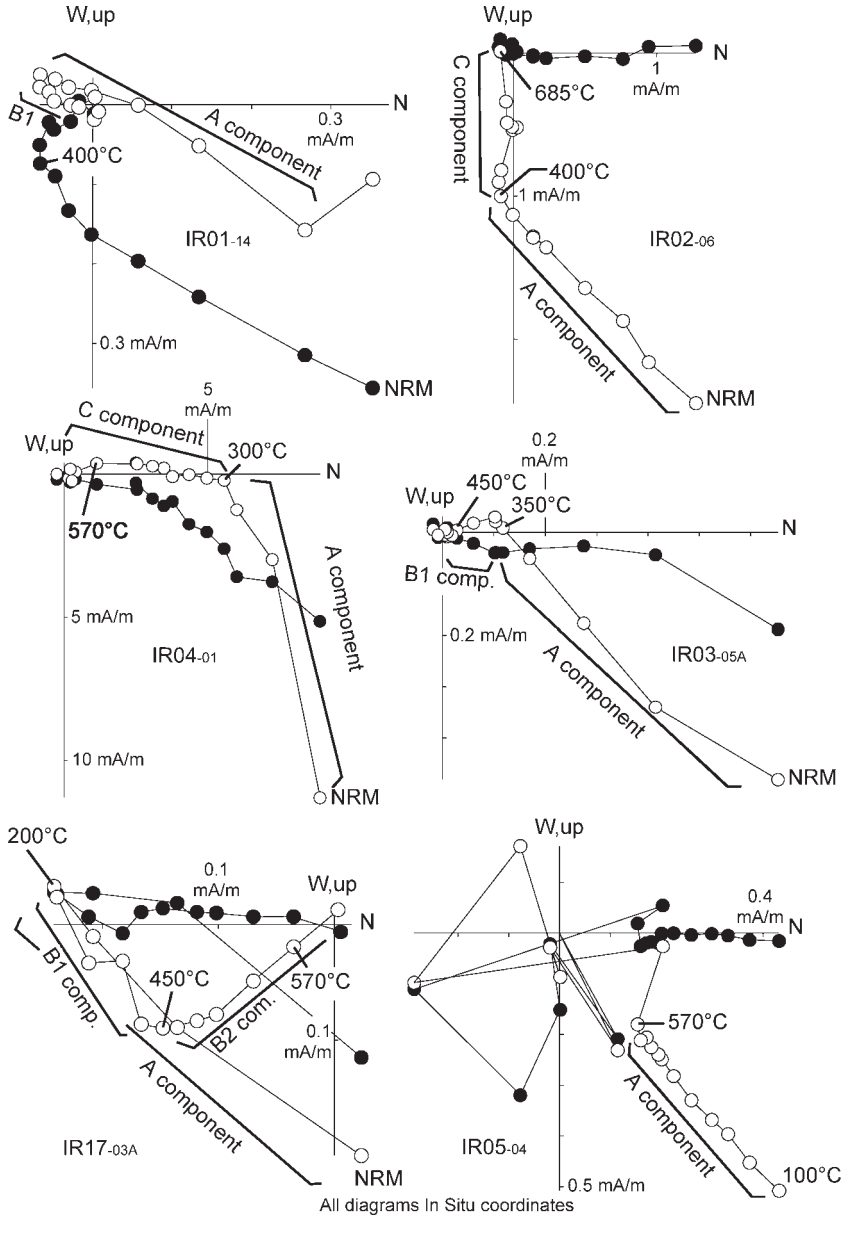

Fig. 6. Vector end-point demagnetization diagrams of representative samples from sites IR01, IR02, IR03, IR04, IR05 and IR17 from Nakhlak with indication of magnetic components isolated. Closed symbols are projections onto the horizontal plane and open symbols onto the vertical plane in *in situ* (geographical) co-ordinates. Demagnetization temperatures are expressed in °C.

post-folding differential rotation on vertical axes within the highly deformed Nakhlak structure.

The drift history of Iran

Several studies have been conducted since the 1970s on Palaeozoic–Cenozoic rock units from Iran. Data from the literature summarized in Van der Voo (1993) and Besse *et al.* (1998), augmented by data from this study, have been used to calculate north palaeomagnetic poles and palaeolatitudes for Iran from the Ordovician to the Triassic (Table 2). In our reconstructions, the various Iranian blocks, e.g. Alborz, Yadz, Tabas, Lut and Sanandaj–Sirjan (Fig. 1), have not been considered separately because the available palaeomagnetic results are too

Table 2. *Summary of palaeomagnetic data from the literature and this study from Iran*

Site	Rock unit	Slat	Slong	Rel.age	L.age	H.age	N	k_{tc}	$\alpha_{95_{tc}}$	Dec.$_{tc}$	Inc.$_{tc}$	NPlat.$_{tc}$	NPlong.$_{tc}$	A95,dp/dm	Plat	errPlat	Reference
IR12	Site IR12, Shirgesht Formation	33.18	53.89	Late Ordovician	460.9	443.7	26[1]	47.2	4.2	263.0	51.8	−12.0	175.0	3.9/5.7	−32	±4	This study
RB	Red beds combined	30.5	57.2	Early Devonian	416.0	397.5	13[2]	18.0	10.1	24.2	−1.3	51.3	196.3	5.1/10.1	−1	±5	Wensink (1983)
GL	Geirud Formation lavas, Alborz Mountains	36	51.5	Earliest Carbon[†]	385.3	318.1	5[2]	380.0	3.9	211.0	67.0	0.0	212.0	5.3/6.5*	−50	±5	Wensink *et al.* (1978)
RL	Ruteh lavas, Alborz Mountains	36.3	52.2	l. Mid Permian[‡]	270.6	260.4	13[1]	–	–	124.7	22.6	19.3	289.9	1.9	−12	±2	Besse *et al.* (1998)
H	Hambast Formation, Shahreza	32.0	52.0	Late Permian	260.4	251.0	31[1]	42.0	4.3	142.0	−4.3	−43.4	109.9	2.2/4.3	−2	±2	Besse *et al.* (1998)
IR27	Site IR27 laterite, Alborz Mountains	35.66	52.40	Late Permian	260.4	249.7	12[1]	18.5	10.4	331.8	−1.3	–	–	–	−1/+1	±5	Muttoni *et al.* (submitted)
HE	Hambast–Elikah formations, Abadeh	30.9	53.2	L. Perm./ Induan	260.4	249.7	101[1]	23.7	2.9	134.5	−15.2	−41.7	124.4	1.5/3.0	−8	±1.5	Gallet *et al.* (2000)
SS_1	Sorkh Shale, sites IR34 + IR35 combined	33.33	57.31	Early Triassic	251.0	245.0	27[1]	36.5	4.6	–	17.6	–	–	–	+9?	±2.5	This study
SS_2	Sorkh Shale	33.3	57.3	Early Triassic	251.0	245.0	5[2]	30.0	14.2	288.9	20.8	–	–	–	+11?[§]	±8	Wensink (1982)
NAK_2	Site IR02, Alam Formation	33.53	53.84	Olenekian	249.7	245.0	11[1]	33.0	8.1	37.7	33.7	53.2	158.4	5.3/9.2	+18	±6	This study
NAK_4	Site IR04, Alam Formation	33.58	53.83	Olenekian	249.7	245.0	14[1]	33.9	6.9	169.5	−41.3	76.5	279.5	5.1/8.4	+24	±5	This study
NAK	Sites IR02 + IR04 combined			Olenekian	249.7	245.0	25[1]	29.0	5.4	–	37.4	–	–	–	+21	±4	This study
W	Waliaband limestone, Abadeh	31.0	52.9	Early Norian	216.5	210.0	35[1]	266.9	4.6	–	51.9	–	–	–	+32.5	±4.5	Besse *et al.* (1998)

Site, palaeomagnetic site abbreviation (in extended form under Rock unit); Slat, latitude of palaeomagnetic site in °N; Slong, longitude of palaeomagnetic site in °E; Rel.age, relative age of palaeomagnetic site (Induan is early Early Triassic, Olenekian is late Early Triassic and Norian is middle Late Triassic); L.age, older limit age of palaeomagnetic site in Ma according to the timescale of Gradstein *et al.* (2004); H.age, younger limit age of palaeomagnetic site in Ma according to the timescale of Gradstein *et al.* (2004); N, number of [1]sites or [2]samples; k_{tc}, Fisher (1953) precision parameter of the palaeomagnetic direction in tilt corrected co-ordinates; $\alpha_{95_{tc}}$, Fisher (1953) angle of half-cone of 95% confidence about the palaeomagnetic direction in tilt-corrected co-ordinates; Dec.$_{tc}$/Inc.$_{tc}$, declination/inclination in tilt-corrected co-ordinates of the palaeomagnetic direction; NPlat.$_{tc}$/NPlong.$_{tc}$, latitude (°N)/longitude (°E) of the palaeomagnetic North pole in tilt-corrected co-ordinates; A95,dp/dm, Fisher (1953) angle of half-cone of 95% confidence (A95) and oval of 95% confidence (dp/dm) about the palaeomagnetic pole in tilt-corrected co-ordinates; Plat, palaeolatitude (°N when positive, °S when negative); errPlat, error of palaeolatitude expressed in degrees (°).

*The oval of confidence reported by Wensink *et al.* (1978, table 2) is 3.9°/5.3°, but if calculated from the mean direction from table 1 in same paper (i.e. Dec. = 211°E, Inc. = 67°, α_{95} = 3.9°) the oval of confidence is 5.3/6.5.

[†]Wensink *et al.* (1978) attributed these lavas to the Upper Devonian–Lower Carboniferous but according to a recent study by Wendt *et al.* (2005), they are most probably earliest Carboniferous in age.

[‡]The Ruteh lavas at Bear Gully are Capitanian (late Middle Permian) in age (Gaetani *et al.* 2009 and references therein).

[§]Wensink (1982) reported a palaeolatitude of 11°S, but because of the substantial lack of constraints on the polarity of magnetization of the Sorkh Shale, a palaeolatitude of 11°N cannot be excluded; the same applies to sites IR34 and IR35 of this study.

sparse to resolve potential palaeolatitude differences among them. In order to compare poles from Iran with coeval poles from Gondwana and Europe, apparent polar wander (APW) paths for West Gondwana (in NW Africa co-ordinates) and Europe have been constructed using selected data from the literature, as illustrated in Table 3. The APW path of Gondwana during the Palaeozoic has been the subject of much debate because some of the paleomagnetic poles for the Silurian and Devonian were derived from suspect terranes from Australia (McElhinny *et al.* 2003 and references therein). The Ordovician–Carboniferous Gondwana APW path adopted in this study is from McElhinny *et al.* (2003), whereas the coeval APW path for Europe is from Van der Voo (1993). The Permian–Triassic segments of the Gondwana and Europe APW paths are derived from palaeomagnetic poles of generally good quality (*sensu* Van der Voo 1993) and are listed in Table 3. Poles for West Gondwana have been rotated from NW Africa into Arabian co-ordinates using an Euler pole derived from Lottes & Rowley (1990) (26.22°N, 11.15°E, $\Omega = 14.17°$), and have been plotted together with the European poles in Figure 7. These poles have been used to calculate Ordovician–Triassic palaeolatitudes expected at a nominal point located at 33°N, 53°E in central Iran for comparison with observed Iranian palaeolatitudes (Fig. 8). Data have been grouped in three time windows: namely, Late Ordovician–Early Carboniferous; Middle Permian–early Early Triassic; and late Early Triassic–Late Triassic.

Late Ordovician–Early Carboniferous: Iran as part of Gondwana

Data from Iran pertaining to this time window come from the Upper Ordovician site IR12 of this study (Fig. 1 and Table 2; site IR12), the Lower Devonian Red beds of Wensink (1983) (site RB) and the Geirud lavas of Wensink *et al.* (1978) (site GL). The Geirud lavas were attributed to the Late Devonian–Early Carboniferous by Wensink *et al.* (1978), but, according to Wendt *et al.* (2005), they are bracketed between upper Famennian sediments below and upper Tournaisian–Visean sediments above, and are therefore probably earliest Carboniferous in age.

The polarity of magnetization at these sites is unknown. Hence, their hemisphere of magnetization acquisition and north palaeomagnetic poles (defined by magnetizations in normal polarity reference frame) cannot be unequivocally determined. Polarity has been chosen in order to obtain the simplest tectonic scenario derived from comparison with coeval north poles from West Gondwana and Europe. Reverse, normal and reverse polarity has been assigned to the mean magnetization of, respectively, the Upper Ordovician site IR12 (Dec. = 263.0°E, Inc. = 51.8°), the Lower Devonian Red beds (Dec. = 24.2°E, Inc. = −1.3°) and the lowermost Carboniferous Geirud lavas (Dec. = 211.0°E, Inc. = 67.0°). The derived palaeomagnetic north poles (Table 2) fall relatively close to, respectively, the Late Ordovician, Early Devonian and Early Carboniferous north poles of West Gondwana (Fig. 7A). This substantial congruence of poles (within palaeomagnetic error resolution) over a period of remarkable polar wander implies significant tectonic coherence of central Iran (sites IR12 and RB) and the Alborz region (site GL) with West Gondwana during this time interval. The sampled sites were located at a palaeolatitude of, respectively, approximately 32°S (±4°) during the Late Ordovician, approximately 1°S (±5°) during the Early Devonian and approximately 50°S (±5°) during the earliest Carboniferous, close to the Arabian margin of West Gondwana (Fig. 8, sites IR12, RB and GL, respectively). These overall conclusions concerning the Arabian affinity of Iran in the Palaeozoic substantiate previous conclusions by Wensink and colleagues (e.g. Wensink *et al.* 1978), and rule out the hypothesis that the Alborz region was located close to the southern margin of Eurasia during the Early Carboniferous as proposed by Kalvoda (2002) using palaeobiogegraphic data.

Middle Permian–early Early Triassic: Iran in motion

Data from Iran pertaining to this time window come from four rock units: the Middle Permian Ruteh lavas from the Alborz Mountains (Besse *et al.* 1998) (Fig. 1 and Table 2, site RL); the Upper Permian Hambast Formation from Shahreza (Besse *et al.* 1998) (site H); the Upper Permian laterite of site IR27 from the Alborz Mountains (this study; Muttoni *et al.* submitted); and the Upper Permian–lower Lower Triassic Hambast and Elikah formations from Abadeh (Gallet *et al.* 2000) (site HE). The Ruteh lavas studied by Besse *et al.* (1998), equivalent to the Ruteh lavas studied by Wensink (1979), have been attributed to the Late Permian following stratigraphic considerations from the literature (Besse *et al.* 1998). In the well-studied Bear Gully section, these lavas are interbedded in the uppermost part of the Ruteh Formation, biostratigraphically dated to the late Middle Permian (Capitanian) (Gaetani *et al.* 2009). A Capitanian age for the Ruteh lavas sampled by Besse *et al.* (1998) is therefore adopted in this study.

Table 3. *Palaeomagnetic reference poles from West Gondwana and Europe*

Age	Long. (°E)	Lat. (°N)	A95 or dp/dm (°)	*K*	*N*	Reference
GONDWANA in NW Africa co-ordinates; rotation poles of Lottes & Rowley (1990)						
Ordovician–Carboniferous						Table 3, McElhinny *et al.* (2003)
Early Permian	242.0	41.4	4.4	122	10	See*
Middle Permian	239.9	44.1				See†
Late Permian–Early Triassic	237.6	46.8	3.1	317	8	Muttoni *et al.* (1996)
Middle Triassic	218.1	57.1	6.3	67	9	Muttoni *et al.* (2001)
Late Triassic–Early Jurassic; based on the following palaeomagnetic poles:						
Bolivar Dykes, Venezuela	206	74	5			MacDonald & Opdyke (1974)
Paramillos, Cach-Uspallata Argentina	223	67	13			Creer *et al.* (1970)
Zambia Red Sandstone	211	72	5			Opdyke (1964)
Atlas & Meseta Volcanic, Morocco	216	71	7			Bardon *et al.* (1973)
Late Triassic–Early Jurassic	214.8	71.1	4.3	458	4	same as in Muttoni *et al.* (1996)
EUROPE						
Ordovician–Carboniferous						Table 5.7 in Van der Voo (1993)
Early Permian	166.2	42.2	3.1	126	18	Muttoni *et al*. (2003, online table 2)
Middle Permian	164.5	46.4				See†
Late Permian–Early Triassic; based on the following palaeomagnetic poles:						
North Sudetic Sed. Zechstein	168	51	4/7			Nawrocki (1997)
Intrasudetic Sed. Zechstein	160	51	2/4			Nawrocki (1997)
Lower Buntsandstein	166	51	3			Szurlies *et al.* (2003)
Buntsandstein Holy Cross	155	49	2			Nawrocki *et al.* (2003)
Saint-Pierre pelites	163	50	5			Diego-Orozco & Henry (1993)

Massif des Maures pelites	161	51	4			Merabet & Daly (1986)
St Affrique sediments	167	50	12			Cogné *et al.* (1993)
Lunner dykes 243 ± 5 Ar/Ar	164	53	6			Torsvik *et al.* (1998)
Late Permian–Early Triassic	162.9	50.8	2.0	764	8	
Middle Triassic; based on the following palaeomagnetic poles:						
Mushelkalk, Silesia	123	53	12			Symons *et al.* (1995)
Gipskeuper, Germany	131	49	6			Edel & Duringer (1997)
Mushelkalk, Poland	143	52	6			Nawrocki & Szulc (2000)
Sherwood Sandstones, UK	139	53	3.5			Hounslow & McIntosh (2003)
Heming Limestone, France	141	53.5	3			Théveniaut *et al.* (1992)
Middle Triassic	135.3	52.4	5.0	234	5	
Late Triassic; based on the following palaeomagnetic poles:						
Rhaetian sediments, Germany, France	112	50	8			Edel & Duringer (1997)
Blue Anchor Formation, UK	109	52	6.5			Hounslow *et al.* (2004)
Mercia Mudstone, UK	128	50	5			Briden & Daniels (1999)
Twyning Formation, UK	114	48	4			Hounslow *et al.* (2004)
Late Triassic	115.9	50.0	6.6	198	4	

Age, relative age of palaeomagnetic pole; Long. (°E), longitude of palaeomagnetic pole in °E; Lat. (°N), latitude of palaeomagnetic pole in °N; A95, dp/dm, Fisher (1953) errors about the palaeomagnetic pole in degrees (°); *K*, Fisher (1953) precision parameter; *N*, number of palaeomagnetic poles used to calculate the overall mean palaeomagnetic pole.

*Palaeomagnetic pole obtained by averaging $N=9$ palaeomagnetic poles listed in Muttoni *et al.* (2003, online table 2) and the palaeomagnetic pole from the Jebel Nehoud ring complex, Sudan (280 ± 2 Ma) of Bachtadse *et al.* (2002).

†Obtained from linear interpolation of bracketing Early Permian and Late Permian–Early Triassic palaeomagnetic poles.

In this table, all West Gondwana palaeomagnetic poles are in NW Africa co-ordinates (Euler poles of rotation from Lottes & Rowley (1990)). In Fig. 7, the West Gondwana overall mean palaeomagnetic poles are plotted in Arabian co-ordinates using a NW Africa to Arabian Euler pole of rotation derived from Lottes & Rowley (1990) (26.22°N, 11.15°E, rotation angle 14.17°).

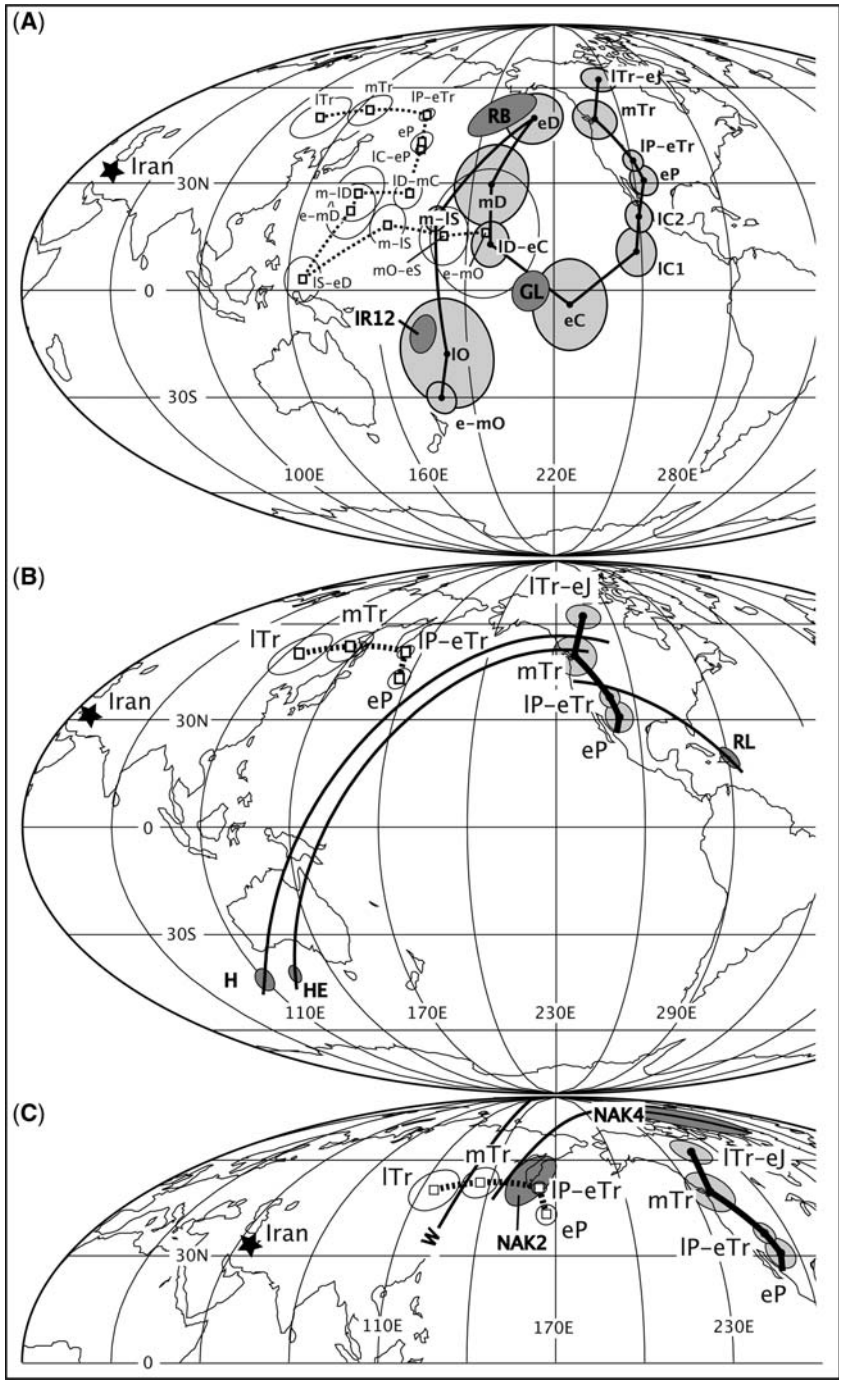

Fig. 7. (**A**) The Ordorician–Triassic APW paths of West Gondwana (Table 3, rotated into Arabian co-ordinates) and Europe (Table 3) are compared with palaeomagnetic poles from Late Ordovician site IR12, the Early Devonian Red beds of Wensink (1983) (RB) and the earliest Carboniferous Geirud lavas of Wensink *et al.* (1978) (GL). The congruence with West Gondwana poles lO (Late Ordovician) eD (Early Devonian) and lD–eC to eC (Late Devonian–Early Carboniferous), respectively, is evident. (**B**) The Permian–Triassic segments of the APW paths of West

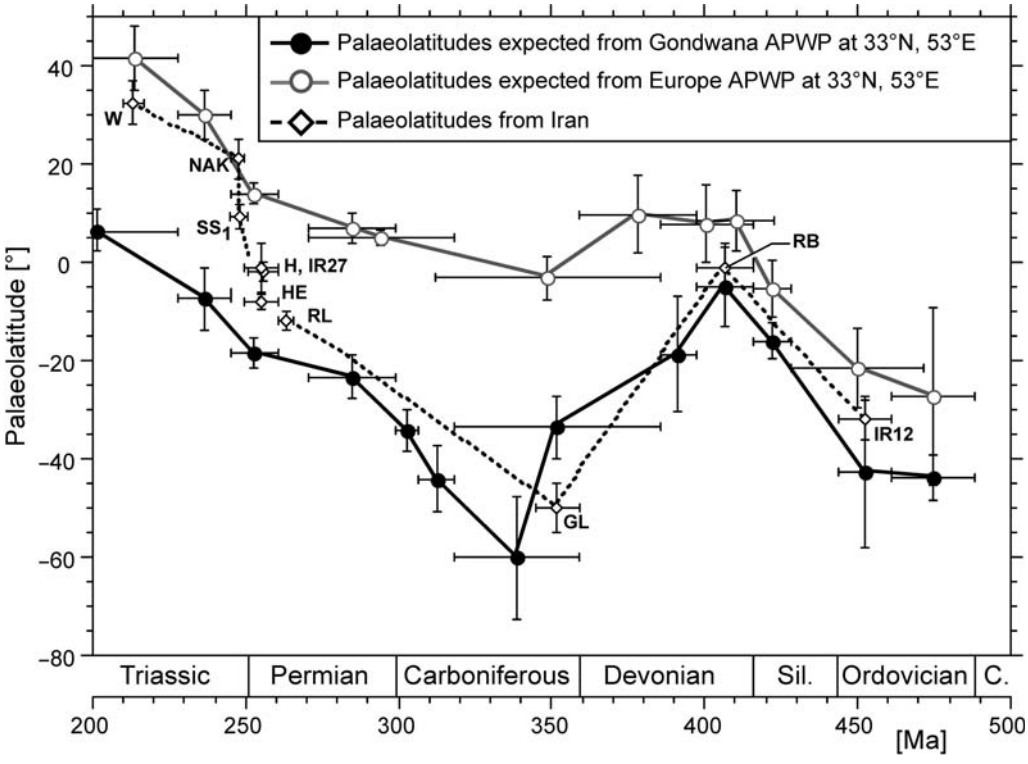

Fig. 8. Palaeolatitudes of the Iranian sites (acronyms and values in Table 2) compared with the palaeolatitudes expected at a nominal site located at 33°N, 53°E in central Iran from the West Gondwana APW path (Table 3, rotated into Arabian co-ordinates) and the Europe APW path (Table 3). Ages according to Gradstein *et al*. (2004).

The polarities of magnetization of the two entries from the Hambast and Elikah formations are known from magnetostratigraphic correlations with sections from the literature of believed known polarity (Besse *et al.* 1998; Gallet *et al.* 2000). Their north palaeomagnetic poles (Fig. 7B, poles H and HE) are significantly displaced with respect to both the West Gondwana and Europe APW paths. This displacement could be owing to variable combinations of plate motion and local vertical-axis tectonic rotations. In order to discriminate between these two sources of displacement, the palaeomagnetic poles have been projected laterally along colatitude small circles, and have been found to intercept younger (Triassic) portions of the West Gondwana APW path (Fig. 7B). This suggests that the observed polar displacement has a main contribution from clockwise vertical-axis tectonic rotations (see also Besse *et al.* 1998) and a subordinate contribution probably from the plate motion of Iran relative to West Gondwana. Clockwise rotations explain the offset between Iran and

Fig. 7. (*Continued*) Gondwana and Europe are compared with palaeomagnetic poles from the late Middle Permian Ruteh lavas and the Late Permian Hambast Formation of Besse *et al.* (1998) (RL and H, respectively), and the Late Permian–early Early Triassic Hambast and Elikah formations of Gallet *et al.* (2000) (HE). Colatitude small circles of poles are indicated. (**C**) The Permian–Triassic segments of the APW paths of West Gondwana and Europe are compared with palaeomagnetic poles and associated colatitude small circles from late Early Triassic sites IR02 and IR04 from Nakhlak (NAK_2 and NAK_4, respectively) and the colatitude small circle of the Upper Triassic (lower Norian) Waliand limestone pole of Besse *et al.* (1998) (W). Age of poles as follows: e–mO, Early–Middle Ordovician; lO, Late Ordovician; mO–eS, Middle Ordovician–Early Silurian; m–lS, Middle–Late Silurian; lS–eD, Late Silurian–Early Devonian; eD, Early Devonian; mD, Middle Devonian; e–mD, Early–Middle Devonian; m–lD, Middle–Late Devonian; lD–eC, Late Devonian–Early Carboniferous; lD–mC, Late Devonian–Middle Carboniferous; eC, Early Carboniferous; lC1, early Late Carboniferous; lC2, late Late Carboniferous; lC–eP, Late Carboniferous–Early Permian; eP, Early Permian; lP–eTr, Late Permian–Early Triassic; mTr, Middle Triassic; lTr, Late Triassic; lTr–eJ, Late Triassic–Early Jurassic.

West Gondwana poles along colatitude small circles, whereas relative plate motion explains the offset between the projected Iran poles and the coeval Late Permian–Early Triassic West Gondwana reference pole. According to this analysis, the sampled units were located at subequatorial palaeolatitudes (*c.* 2°S ± 2° for site H; *c.* 8°S ± 1.5° for site HE; Table 2) north of the Arabian margin of West Gondwana in Late Permian–early Early Triassic times (Fig. 8, sites H and HE), whereas the timing of post-depositional clockwise rotation is at present difficult to ascertain. Similar conclusions can also be drawn for the Upper Permian laterite of site IR27. Here, polarity is unknown. Hence, hemisphere of magnetization, and sense and amount of tectonic rotation, cannot be unequivocally determined. However, this constitutes a negligible problem in view of the fact that the characteristic magnetizations therein isolated clearly indicate equatorial palaeolatitudes of either approximately 1°S or approximately 1°N (±5°) (Table 2, site IR27). This also suggests that the Alborz region, within which site IR27 is located, was already detached from the Arabian margin in Late Permian times (Fig. 8, site IR27).

The notion derived from the present analysis that the Iranian block(s) had Arabian affinity in the Late Ordovician–earliest Carboniferous and were drifting to the north with respect to Arabia, attaining subequatorial palaeolatitudes in the Late Permian–early Early Triassic, is used to interpret the hemisphere of magnetization acquisition of the late Middle Permian Ruteh lavas, the polarity of which is unknown. The simplest scenario is to assign reverse polarity to its mean magnetization (Dec. = 124.7°E, Inc. = 22.6°; Table 2). The derived north palaeomagnetic pole is rotated counterclockwise with respect to the West Gondwana polar wander path, and its colatitude small circle intercepts slightly younger portions of the same path (Fig. 7B, pole RL). This implies similar conclusions as those for the Hambast and Elikah formations, i.e. that the observed polar displacement can be accounted for by a combination of vertical-axis tectonic rotations and plate motion. The Alborz region, within which the Ruteh lavas are located, resided at a palaeolatitude of approximately 12°S ± 2° (Table 2, site RL), slightly to the north of the Arabian margin in late Middle Permian times (Fig. 8, site RL).

Late Early Triassic–Late Triassic: Iran approaching Europe

Data from Iran pertaining to this time window come from the characteristic components of Lower Triassic sites IR34 and IR35 from the Sorkh Shale of this study and Wensink (1982) (Fig. 1 and Table 2, site SS), upper Lower Triassic (Olenekian) sites IR02 and IR04 of this study (site NAK), and the Upper Triassic (lower Norian) Waliaband limestone of Besse *et al.* (1998) (site W).

According to the previous analysis, the Iranian block(s) moved northwards from the southern hemisphere to subequatorial palaeolatitudes during the Permian–early Early Triassic. Hence, the simplest scenario is to envisage a continuation of this northwards motion into the northern hemisphere during the Triassic. Polarity has been assigned to the mean characteristic components of sites IR02 and IR04 according to a northern hemisphere origin of magnetization, and was used to calculate north palaeomagnetic poles (Fig. 7C and Table 2; NAK_2 and NAK_4, respectively). Pole NAK_2 falls very close to the Late Permian–Early Triassic reference pole of Europe. Pole NAK_4 is rotated counterclockwise with respect to the APW path of Europe, and, when traced laterally along a colatitude small circle, it falls close to the Late Permian–Early Triassic reference pole of Europe, where pole NAK_2 is also located (Fig. 7C). This suggests substantial European affinity of the sampled units and local vertical-axis tectonic rotations of the eastern part of the Nakhlak structure where site IR04 is located. A palaeolatitude of approximately 21°N ± 4° is derived by combining inclination-only data from both sites (Table 2, pole NAK). This palaeolatitude places the sampled units close to the European margin in late Early Triassic (Olenekian) times (Fig. 8, pole NAK). In a recent analysis, Bagheri & Stampfli (2008) interpreted the Naklakh–Anarak area as part of a 'Variscan accretionary complex' pertaining to the Turan domain. If this were the case, the European palaeolatitudes from the Naklakh structure would not be utilizable for the definition of the younger part of the Cimmerian drift history outlined in this study.

Data from the Early Triassic Sorkh Shale are more difficult to interpret in terms of hemisphere of magnetization acquisition. Inclination-only data from combined sites IR34 and IR35 indicate a palaeolatitude of approximately 9° ± 2.5° (Table 2, site SS_1). Wensink (1982) reported a similar palaeolatitude (*c.* 11° ± 8°) for Sorkh Shale sites from the same general area of this study, and opted for a southern hemisphere origin of deposition (*c.* 11°S). The substantial lack of constraints on the polarity of magnetization does not preclude, however, a northern hemisphere palaeolatitude, as suggested by Besse *et al.* (1998). The general drift trend of the Iranian block(s), as described above, is of moderate help in discerning between the two options. Palaeolatitudes from the Hambast and Elikah formations and site IR27 span from approximately 8°S to equatorial in the Late Permian–early Early Triassic; late Early Triassic palaeolatitudes from Nakhlak are in the

order of about 21°N. Palaeolatitudes from the Sorkh Shale are tentatively interpreted as pertaining to the northern hemisphere, in agreement with Besse *et al.* (1998) (Fig. 8, site SS_1), although caution on this interpretation should be maintained essentially because of the poor age constraints of the sampled units.

Finally, Besse *et al.* (1998) showed the presence, in sites from the Upper Triassic (lower Norian) Waliaband limestone at Abadeh, of pre-folding

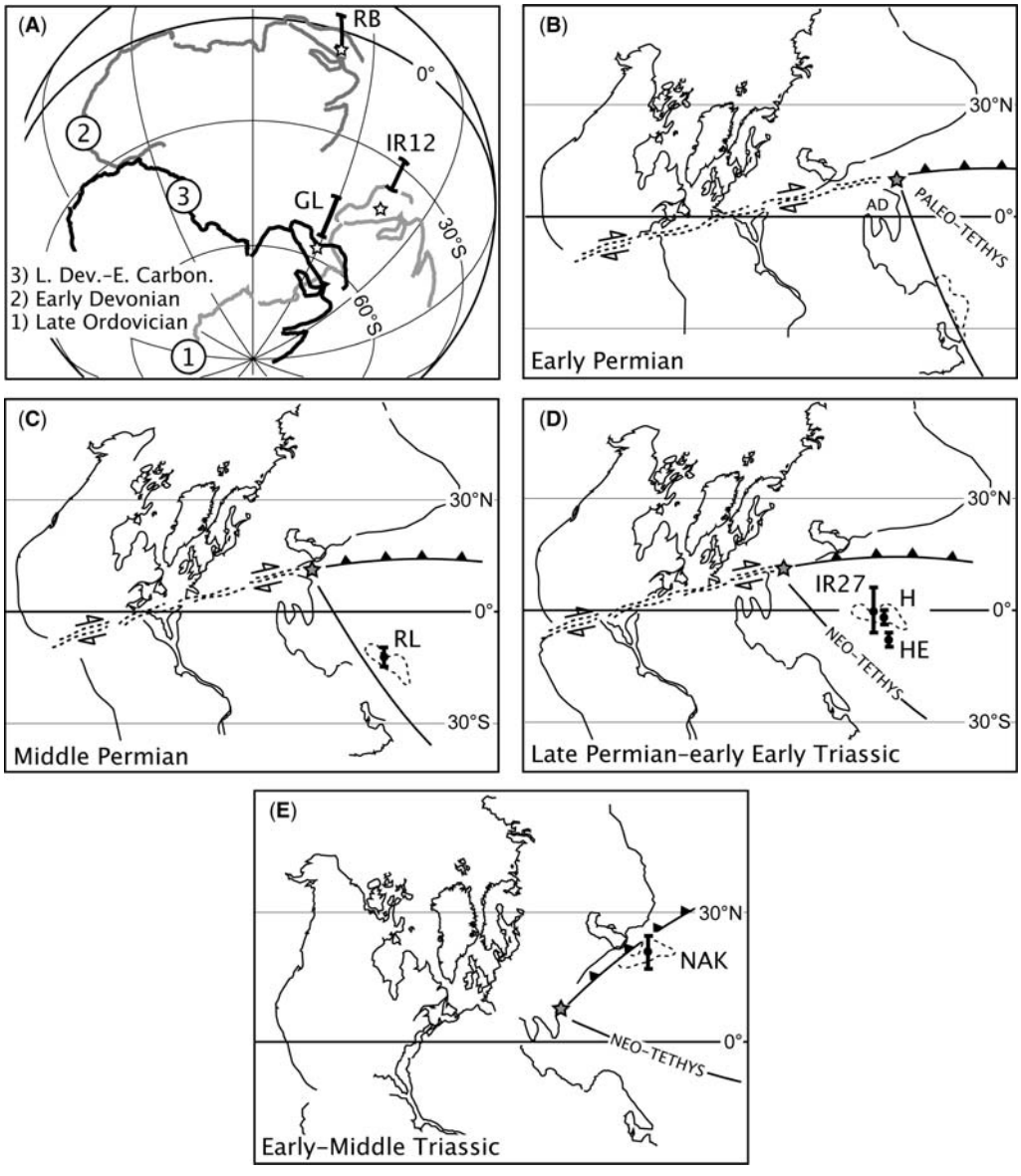

Fig. 9. Palaeomagnetic-based palaeogeographic reconstruction of West Gondwana and Pangaea over (**A**) the Late Ordovician, Early Devonian and Late Devonian–Early Carboniferous (**B**) Early Permian, (**C**) Middle Permian, (**D**) Late Permian–early Early Triassic and (**E**) Early–Middle Triassic, obtained using palaeomagnetic poles from West Gondwana and Europe (Table 3). Africa is internally treated as three plates (NW, NE and S Africa), with Adria (AD in panel B) tectonically coherent with NW Africa (Muttoni *et al.* 2003). Internal Gondwana plates are reconstructed using Euler poles of Lottes & Rowley (1990). Internal Laurasia plates are reconstructed using Euler poles of Bullard *et al.* (1965). Palaeolatitudes from Iranian sites discussed in the text and summarized in Table 2 are indicated by error bars and associated acronyms. Reconstructions made with PaleoMac 6.1 (Cogné 2003).

palaeomagnetic directions variably rotated about vertical axes. Their analysis of inclination-only data produced an overall mean inclination value of 51.9° ($\alpha_{95} = 4.6°$; Table 2). By assigning normal polarity to this mean inclination, according to a northern hemisphere origin of magnetization acquisition, a colatitude small circle containing the north palaeomagnetic pole has been calculated. This small circle intersects the Middle–Late Triassic portion of the European APW path (Fig. 7C, small circle W) suggesting European affinity for the Waliaband limestone, as originally proposed by Besse *et al.* (1998). These sites resided at a palaeolatitude of approximately 32.5°N ± 4.5°, close to the European margin in early Norian times (Fig. 8, small circle W).

In conclusion, data from this study and the literature suggest that the Iranian block(s) were located close to the Arabian margin of Gondwana in the Late Ordovician–earliest Carboniferous. They have drifted off this margin since the Permian, attained subequatorial palaeolatitudes at Late Permian–early Early Triassic times and approached the Eurasian margin by the late Early Triassic. From then on, the Iranian block(s) maintained European affinity, as deduced from early Norian data and, more generally, from Jurassic–Cretaceous data (e.g. Garedu Red beds, Bidou Beds and Dehuk Sandstones; Wensink 1982), as extensively discussed in Besse *et al.* (1998).

Palaeogeography

The drift history of Iran, outlined in the previous section, has been placed in a general palaeogeographical context by reconstructing the configuration of continents using palaeomagnetic poles from West Gondwana and Europe (Table 3) and Euler poles from the literature (Fig. 9). According to the Ordovician–Carboniferous Gondwana APW path of McElhinny *et al.* (2003), the Arabian margin as part of Africa experienced significant plate motion, drifting from high southern latitudes in the Late Ordovician to subequatorial latitudes in the Early Devonian, and back to intermediate southern latitudes in the Late Devonian–Early Carboniferous (Fig. 9A). As anticipated in the previous section, Iran tracked closely this motion. The palaeolatitudes expected from the West Gondwana reference palaeopoles at Late Ordovician site IR12, Early Devonian site RB (Red beds) and earliest Carboniferous site GL (Geirud lavas) (Fig. 9A, stars) are in relatively close congruence with the palaeolatitudes calculated from the respective characteristic magnetizations (Fig. 9A, error bars). In the Carboniferous, Gondwana and Laurasia coalesced to form Pangaea. The Early Permian and Late Permian–Early Triassic Pangaea reconstructions of Figure 9B, D, virtually identical to those of Muttoni *et al.* (2003), bracket a Middle Permian reconstruction (Fig. 9C) obtained by linear interpolation of Early Permian and Late Permian–Early Triassic poles of Table 3. At these times, palaeomagnetic data reveal a grand-scale tectonic scenario consisting of a transformation of Pangaea from an Irvingian B configuration (Irving 1977) in the Early Permian to a Wegenerian A-type configuration by the Late Permian–Early Triassic, as extensively discussed in Muttoni *et al.* (2003 and references therein). This transformation is coeval with the onset of northward drift of the Iranian block(s) across the Palaeotethys by way of Neotethys opening, depicting altogether an internally consistent plate motion scenario that is the subject of a parallel paper (Muttoni *et al.* submitted). Key elements of this northward drift are palaeolatitude estimates from the late Middle Permian Ruteh lavas (RL), the Late Permian–early Early Triassic Hambast and Elikah formations (H, HE), and the Late Permian site IR27 (Fig. 9C, D). Finally, palaeolatitudes from the late Early Triassic sites IR02 and IR04 from Nakhlak support an incipient approach of the Iranian block(s) with the active margin of Eurasia in the frame of an Early–Middle Triassic Pangaea configuration of the A-type (Fig. 9E, NAK).

Conclusions

Palaeomagnetic data from this study and the literature have been used to reconstruct the drift history of the Iranian block(s) from the Ordovician to the Triassic. Key elements of this reconstruction are:

- a robustly determined palaeomagnetic affinity of Iran with Arabia (Gondwana) during the Late Ordovician–earliest Carboniferous;
- clear palaeomagnetic evidence for the residence of Iran on subequatorial palaeolatitudes during the Late Permian–early Early Triassic, noticeably disengaged from both the parental Gondwanan margin in the southern hemisphere and the espousal Laurasian margin in the northern hemisphere.

On these two elements is based the interpretation of pre-Late Permian latitudes from Iran as pertaining to the southern hemisphere, and post-early Early Triassic latitudes as pertaining to the northern hemisphere. The resulting scenario is that of a relatively rapid northward drift that brought the Iranian block(s) to cover approximately 2500–3000 km of Palaeotethys in about 35 Ma (from *c.* 280 Ma in the Early Permian to *c.* 245 Ma at the end of the late Early Triassic), at an average plate speed of approximately 7–8 cm year^{-1}. This motion was largely coeval to, and kinematically linked with,

the transformation of Pangaea from an Irvingian B to a Wegenerian A-type configuration (Muttoni *et al.* 2003, submitted).

The spatio-temporal resolution of the observed northward drift does not allow distinguishing components of relative motion between crustal blocks (e.g. Alborz v. Tabas v. Sanandaj–Sirjan). Despite these and other uncertainties (e.g. the possible Turanian rather than Cimmerian affinity of Naklakh: Bagheri & Stampfli 2008), the overall drift history outlined above is in broad agreement with geological data. Several authors pointed out the Proterozoic–Palaeozoic Gondwanan ancestry of north and central Iran based on the nature of their basement and the overlying sedimentary succession (Stöcklin 1968, 1974; Berberian & King 1981; Wendt *et al.* 2005). Zanchi *et al.* (2009*b*) pointed out that north and central Iran are entirely located south of the Eo-Cimmerian belt, which marks the collision of Iran with the southern Eurasian margin (e.g. Sengör 1990; Zanchi *et al.* 2006). The upper age limit of this collision is Late Triassic, as the Upper Triassic–Middle Jurassic Shemshak Group seals unconformably Eo-Cimmerian structures affecting the Palaeozoic–Middle Triassic sequences of northern Alborz (Zanchi *et al.* 2006).

In this paper we opted to avoid discussing palaeomagnetic directions in terms of tectonic rotations within the assorted Iranian fold-and-thrust belts, a subject exhaustively treated by Besse *et al.* (1998). Nevertheless, our data from Nakhlak advise caution with regard to the hypothesis by Soffel *et al.* (1996) that a 135° counterclockwise block rotation has occurred between the internal part of central Iran and Europe since the Middle Triassic, an hypothesis that is based on sparse data from the Triassic sequence of Nakhlak. Multiple remagnetization events pervasively overprinted the volcanoclastic sandstones and siltstones at Nakhlak, whereas magnetization components of presumed primary age were observed only in a solitary nodular limestone interval. These primary components, when compared with reference European directions, suggest no rotation of the western part of the Nakhlak structure (site IR02) and a moderate counterclockwise rotation of the eastern part of the Nakhlak structure since the late Early Triassic (site IR04). A complex and largely poorly known pattern of tectonic rotations around vertical axes has been active in central Iran since the Neogene (Walker & Jackson 2004) as a consequence of crustal-scale north–south shearing. Undoubtedly, more data are required to unravel in detail the complex tectonic history of Iran, a country of over 1.6×10^6 km^2 and less than 30 palaeomagnetic entries listed in the IAGA Global Palaeomagnetic Database 2007.

The MEBE (Middle East Basin Evolution) Programme funded the field work. Helpful comments by reviewers J. Tait and V. Bachtadse improved the manuscript. We thank M.-F. Brunet and J. Granath for assistance during preparation of this manuscript.

References

ALLEN, M. B., GHASSEMI, M. R., SHAHRABI, M. & QORASHI, M. 2003. Accommodation of late Cenozoic oblique shortening in the Alborz range, northern Iran. *Journal of Structural Geology*, **25**, 659–672.

ANGIOLINI, L., GAETANI, M., MUTTONI, G., STEPHENSON, M. H. & ZANCHI, A. 2007. Tethyan oceanic currents and climate gradients 300 m.y. ago. *Geology*, **35**, 1071–1074.

BACHTADSE, V., ZANGLEIN, R., TAIT, J. & SOFFEL, H. 2002. Palaeomagnetism of the Permo/Carboniferous (280 Ma) Jebel Nehoud ring complex, Kordofan, Central Sudan. *Journal of African Earth Sciences*, **35**, 89–97.

BAGHERI, S. & STAMPFLI, G. M. 2008. The Anarak, Jandaq and Posht-e-Badam metamorphic complexes in central Iran: New geological data, relationships and tectonic implications. *Tectonophysics*, **451**, 123–155.

BALINI, M. *ET AL*. 2009. The Triassic stratigraphic succession of Nakhlak (Central Iran), a record from an active margin. *In*: BRUNET, M.-F., WILMSEN, M. & GRANATH, J. W. (eds) *South Caspian to Central Iran Basins*. Geological Society, London, Special Publications, **312**, 287–321.

BARDON, C., BOSSERT, A., HAMZEH, R., ROLLEY, J.-P. & WESTPHAL, M. 1973. Etude paléomagnétique de formations volcaniques du Crétacé inférieur dans l'Atlas de Beni Mellal (Maroc). *Comptes rendus de l'Académie des Sciences Paris*, **277**, 2141–2144.

BERBERIAN, M. & KING, G. 1981. Toward a paleogeography and tectonic evolution of Iran. *Canadian Journal of Earth Sciences*, **18**, 210–265.

BESSE, J., TORCQ, F., GALLET, Y., RICOU, L. E., KRYSTYN, L. & SAIDI, A. 1998. Late Permian to Late Triassic palaeomagnetic data from Iran: constraints on the migration of the Iranian block through the Tethys Ocean and initial destruction of Pangaea. *Geophysical Journal International*, **135**, 77–92.

BRIDEN, J. C. & DANIELS, B. A. 1999. Palaeomagnetic correlation of the Upper Triassic of Somerset, England, with continental Europe and eastern North America. *Journal of the Geological Society, London*, **156**, 317–326.

BRÖNNIMANN, P., ZANINETTI, L., MOSHTAGHIAN, A. & HUBER, H. 1973. Foraminifera from the Sorkh Shale Formation of the Tabas area, east-central Iran. *Rivista Italiana di Paleontologia e Stratigrafia*, **79**, 1–32.

BULLARD, E. C., EVERETT, J. E. & SMITH, A. G. 1965. A symposium on continental drift. IV. The fit of the continents around the Atlantic. *Philosophical Transactions of the Royal Society of London*, **A258**, 41–51.

COGNÉ, J.-P. 2003. PaleoMac: a Macintosh™ application for treating paleomagnetic data and making plate reconstructions. *Geochemistry, Geophysics and Geosystems*, **41**, 1007.

COGNÉ, J.-P., VAN DEN DRIESSCHE, J. & BRUN, J.-P. 1993. Syn-extension rotations in the Permian basin of St Affrique (Massif Central, France): paleomagnetic constraints. *Earth and Planetary Science Letters*, **115**, 29–42.

CREER, K. M., EMBLETON, B. J. J. & VALENCIO, D. A. 1970. Triassic and Permo-Triassic palaeomagnetic data for S. America. *Earth and Planetary Science Letters*, **8**, 173–178.

DIEGO-OROZCO, A. & HENRY, B. 1993. Palaeomagnetic results from the Permian Saint-Affrique basin (France) and implications for late and post-Hercynian tectonics. *Tectonophysics*, **227**, 31–47.

EDEL, J. B. & DURINGER, P. 1997. The apparent polar wander path of the European plate in Upper Triassic–Lower Jurassic times and the Liassic intraplate fracturing of Pangaea: new palaeomagnetic constraints from NW France and SW Germany. *Geophysical Journal International*, **128**, 331–344.

FISHER, R. A. 1953. Dispersion on a sphere. *Proceedings of the Royal Society of London*, **A217**, 295–305.

GAETANI, M., ANGIOLINI, L. *ET AL*. 2009. Pennsylvanian–Early Triassic stratigraphy in the Alborz Mountains (Iran). *In*: BRUNET, M.-F., WILMSEN, M. & GRANATH, J. W. (eds) *South Caspian to Central Iran Basins*. Geological Society, London, Special Publications, **312**, 79–128.

GALLET, Y., KRYSTYN, L., BESSE, J., SAIDI, A. & RICOU, L.-E. 2000. New constraints on the Upper Permian and Lower Triassic geomagnetic polarity timescale from the Abadeh section (central Iran). *Journal of Geophysical Research*, **105**, 2805–2815.

GRADSTEIN, F. M., OGG, J. G. & SMITH, A. G. (eds). 2004. *A Geologic Time Scale 2004*. Cambridge University Press, Cambridge.

HOUNSLOW, M. W. & MCINTOSH, G. 2003. Magnetostratigraphy of the Sherwood Sandstone Group (Lower and Middle Triassic), south Devon, UK: detailed correlation of the marine and non-marine Anisian. *Palaeogeography, Palaeoclimatology, Palaeoecology*, **193**, 325–348.

HOUNSLOW, M. W., POSEN, P. E. & WARRINGTON, G. 2004. Magnetostratigraphy and biostratigraphy of the Upper Triassic and lowermost Jurassic succession, St. Audrie's Bay, UK. *Palaeogeography, Palaeoclimatology, Palaeoecology*, **213**, 331–358.

IRVING, E. 1977. Drift of the major continental blocks since the Devonian. *Nature*, **270**, 304–309.

KALVODA, J. 2002. *Late Devonian–Early Carboniferous Foraminiferal Fauna: Zonations, Evolutionary Events, Paleobiogeography and Tectonic Implications*. Folia, Geologia, **39**, Masaryk University, Brno, Czech Republic.

KIRSCHVINK, J. L. 1980. The least-squares line and plane and the analysis of palaeomagnetic data. *Geophysical Journal of the Royal Astronomical Society*, **62**, 699–718.

LOTTES, A. L. & ROWLEY, D. B. 1990. Reconstruction of the Laurasian and Gondwanan segments of Permian Pangaea. *In*: MCKERROW, W. S. & SCOTESE, C.R. (eds) *Palaeozoic Palaeogeography and Biogeography*. Geological Society of London, Memoir, **12**, 383–395.

LOWRIE, W. 1990. Identification of ferromagnetic minerals in a rock by coercivity and unblocking temperature properties. *Geophysical Research Letters*, **17**, 159–162.

MACDONALD, W. D. & OPDYKE, N. D. 1974. Triassic paleomagnetism of northern South America. *AAPG Bulletin*, **58**, 208–215.

MCELHINNY, M. W., POWELL, C. M. & PISAREVSKY, S. A. 2003. Paleozoic terranes of eastern Australia and the drift history of Gondwana. *Tectonophysics*, **362**, 41–65.

MCFADDEN, P. L. & REID, A. B. 1982. Analysis of palaeomagnetic inclination data. *Geophysical Journal of the Royal Astronomical Society*, **69**, 307–319.

MERABET, N. & DALY, L. 1986. Détermination d'un pole paléomagnétique et mise en évidence d'aimantations à polarité normale sur les formations du Permien supérieur du Massif des Maures (France). *Earth and Planetary Science Letters*, **80**, 156–166.

MUTTONI, G., GAETANI, M., KENT, D. V. *ET AL*. Neotethys opening and the Pangea B to Pangea A transformation during the Permian. *GeoArabia*, submitted.

MUTTONI, G., GARZANTI, E., ALFONSI, L., CIRILLI, S., GERMANI, D. & LOWRIE, W. 2001. Motion of Africa and Adria since the Permian: paleomagnetic and paleoclimatic constraints from northern Libya. *Earth and Planetary Science Letters*, **192**, 159–174.

MUTTONI, G., KENT, D. V. & CHANNELL, J. E. T. 1996. Evolution of Pangea: Paleomagnetic constraints from the Southern Alps, Italy. *Earth and Planetary Science Letters*, **140**, 97–112.

MUTTONI, G., KENT, D. V., GARZANTI, E., BRACK, P., ABRAHAMSEN, N. & GAETANI, M. 2003. Early Permian Pangea 'B' to Late Permian Pangea 'A'. *Earth and Planetary Science Letters*, **215**, 379–394.

NAWROCKI, J. 1997. Permian to Early Triassic magnetostratigraphy from the Central European Basin in Poland: Implications on regional and worldwide correlations. *Earth and Planetary Science Letters*, **152**, 37–58.

NAWROCKI, J. & SZULC, J. 2000. The Middle Triassic magnetostratigraphy from the Peri-Tethys basin in Poland. *Earth and Planetary Science Letters*, **182**, 77–92.

NAWROCKI, J., KULETA, M. & ZBROJA, S. 2003. Buntsandstein magnetostratigraphy from the northern part of the Holy Cross Mountains. *Geological Quarterly*, **47**, 253–260.

OPDYKE, N. D. 1964. The paleomagnetism of some Triassic red beds from Northern Rhodesia. *Journal of Geophysical Research*, **69**, 2495–2497.

SCHALLREUTER, R., HINZ-SCHALLREUTER, I., BALINI, M. & FERRETTI, A. 2006. Late Ordovician Ostracoda from Iran and their significance for palaeogeographical reconstructions. *Zeitschrift für Geologische Wissenschaften*, **34**(5–6), 293–345.

SENGÖR, A. M. C. 1979. Mid-Mesozoic closure of Permo-Triassic Tethys and its implications. *Nature*, **279**, 590–593.

SENGÖR, A. M. C. 1990. A new model for the late Palaeozoic–Mesozoic tectonic evolution of Iran and

implications for Oman. *In*: ROBERTSON, A. H., SEARLE, M. P. & RIES, A. C. (eds) *The Geology and Tectonics of the Oman Region*. Geological Society, London, Special Publications, **49**, 797–831.

SHARKOVSKI, M., SUSOV, M. & KRIVYAKIN, B. 1984. *Geology of the Anarak Area (Central Iran). Explanatory Text of the Anarak Quadrangle Map*. Geological Survey of Iran, **19**.

SOFFEL, H. C., DAVOUDZADEH, M., ROLF, C. & SCHMIDT, S. 1996. New palaeomagnetic data from Central Iran and a Triassic palaeoreconstruction. *Geologische Rundschau*, **85**, 293–302.

STÖCKLIN, J. 1968. Structural history and tectonics of Iran: a review. *AAPG Bulletin*, **52**, 1229–1258.

STÖCKLIN, J. 1974. Possible ancient continental margins in Iran. *In*: BURK, C. A. & DRAKE, C. L. (eds) *The Geology of Continental Margins*. Springer, Berlin, 873–887.

SYMONS, D. T. A., SANGSTER, D. F. & LEACH, D. L. 1995. A Tertiary age from paleomagnetism for Mississippi Valley-type zinc–lead mineralization in Upper Silesia, Poland. *Economic Geology*, **90**, 782–794.

SZURLIES, M., BACHMANN, G. H., MENNING, M., NOWACZYK, N. R. & KÄDING, K.-C. 2003. Magnetostratigraphy and high-resolution lithostratigraphy of the Permian–Triassic boundary interval in Central Germany. *Earth and Planetary Science Letters*, **212**, 263–278.

THÉVENIAUT, H., BESSE, J., EDEL, J. B., WESTPHAL, M. & DURINGER, P. 1992. A Middle Triassic Paleomagnetic Pole for the Eurasian Plate from Heming (France). *Geophysical Research Letters*, **19**, 777–780.

TORSVIK, T. H., EIDE, E. A., MEERT, J. G., SMETHURST, M. A. & WALDERHAUG, H. J. 1998. The Oslo rift: new palaeomagnetic and $^{40}Ar/^{39}Ar$ age constraints. *Geophysical Journal International*, **135**, 1045–1059.

VAN DER VOO, R. 1993. *Paleomagnetism of the Atlantic, Tethys and Iapetus Oceans*. Cambridge University Press, Cambridge.

WALKER, R. & JACKSON, J. 2004. Active tectonics and late Cenozoic strain distribution in central and eastern Iran. *Tectonics*, **23**, TC5010, doi:10.1029/2003TC001529.

WENDT, J., KAUFMANN, B., BELKA, Z., FARSAN, N. & BAVANDPUR, A. K. 2005. Devonian/Lower Carboniferous stratigraphy, facies patterns and palaeogeography of Iran Part II. Northern and central Iran. *Acta Geologica Polonica*, **55**, 31–97.

WENSINK, H. 1979. The implications of some palaeomagnetic data from Iran for its structural history. *Geologie en Mijnbouw*, **58**, 175.

WENSINK, H. 1982. Tectonic inferences of paleomagnetic data from some Mesozoic formations in Central Iran. *Journal of Geophysics*, **51**, 12–23.

WENSINK, H. 1983. Paleomagnetism of red beds of Early Devonian age from Central Iran. *Earth and Planetary Science Letters*, **63**, 325–334.

WENSINK, H., ZIJDERVELD, J. D. A. & VAREKAMP, J. C. 1978. Paleomagnetism and ore mineralogy of some basalts of the Geirud formation of Late Devonian to Early Carboniferous age from southern Alborz, Iran. *Earth and Planetary Science Letters*, **41**, 441–450.

ZANCHI, A., BERRA, F., MATTEI, M., GHASSEMI, M. & SABOURI, J. 2006. Inversion tectonics in Central Alborz, Iran. *Journal of Structural Geology*, **28**, 2023–2037.

ZANCHI, A. *ET AL*. 2009*a*. The Cimmerian evolution of the Nakhlak–Anarak area, Central Iran, and its bearing for the reconstruction of the history of the Eurasian margin. *In*: BRUNET, M.-F., WILMSEN, M. & GRANATH, J. W. (eds) *South Caspian to Central Iran Basins*. Geological Society, London, Special Publications, **312**, 261–286.

ZANCHI, A. *ET AL*. 2009*b*. The Eo-Cimmerian (Late? Triassic) orogeny in North Iran. *In*: BRUNET, M.-F., WILMSEN, M. & GRANATH, J. W. (eds) *South Caspian to Central Iran Basins*. Geological Society, London, Special Publications, **312**, 31–55.

ZIJDERVELD, J. D. A. 1967. A.C. demagnetization of rocks – analysis of results. *In*: COLLINSON, D. W., CREER, K. M. & RUNCORN, S. K. (eds) *Methods in Paleomagnetism*. Elsevier, New York, 254–286.